Wind loads on low-rise buildings – effects of roof geometry

K J Eaton, J R Mayne and N J Cook

Building Research Station

BUILDING
RESEARCH
ESTABLISHMENT
Department of the Environment

Current papers

Current Papers are circulated to selected audience groups appropriate to each subject. Full details of all recent Current Papers and other BRE Publications are published quarterly in BRE NEWS. Requests for BRE NEWS or for placing on the Current Paper mailing list should be addressed to:

Distribution Unit,
Application Services Division,
Building Research Establishment,
Garston, Watford, WD2 7JR.

Extra copies of this paper are available; charge may be made for supplies in quantity

WIND LOADS ON LOW-RISE BUILDINGS - EFFECTS OF ROOF GEOMETRY

K J Eaton, BSc(Eng), PhD, CEng, FRMetS, MIStructE, J R Mayne, BSc and
N J Cook, BSc(Eng), PhD

This paper was presented at 4th International Conference on Wind Effects on Buildings and Structures, London, 8-12 September 1975, and will subsequently appear in the Proceedings

This paper describes the measurement of wind pressures on low-rise buildings at Aylesbury. The pressures were recorded simultaneously at over one hundred positions divided between seven houses in an estate and a specially constructed experimental building situated on open ground adjoining the estate. A unique feature of the experimental building was that the roof pitch could be quickly varied to any angle between 5^{o} and 45^{o}. It was therefore possible to investigate the variation of pressure distributions over the surfaces of the building, and data are presented for two skew wind directions. Initial comparisons have been made with results obtained using models in the Building Research Establishment's boundary layer wind tunnel; time has not permitted a complete series of tests, but preliminary findings from both the full-scale and wind tunnel data are discussed. In particular, the presentation of peak-factor data is extensively covered. Finally, the implications of the results for design purposes are considered and one of the conclusions is that local suction values around the perimeter of low-pitched roofs need increasing in the United Kingdom wind-loading code.

Building Research Establishment
Building Research Station
Garston
Watford
WD2 7JR

NOTATION

C_p = pressure coefficient, $C_{\bar{p}}$ or $C_{\hat{p}}$ as appropriate

$C_{\bar{p}}$ = mean pressure coefficient = $\bar{p}/\bar{q}_{10}$

$C_{\hat{p}}$ = peak pressure coefficient = $\hat{p}_{(1/32)}/\hat{q}_{10}$

C_{σ_p} = $\sigma_p/\bar{q}_{10}$

g = peak-factor = $(\hat{p}_t - \bar{p})/\sigma_p$

h = height of building to the ridge

$\bar{p}$ = mean pressure over record length

$\hat{p}_t$ = maximum or minimum peak pressure as appropriate, the suffix, if added, denoting the dependence of the peak value upon averaging time

$\bar{q}_{10}$ = dynamic pressure based on $\bar{u}_{10}$

$\hat{q}_{10}$ = dynamic pressure based on $\hat{u}_{10}$

t = gust averaging time

$\bar{u}_{10}$ = mean velocity at 10 m over record length

$\hat{u}_{10}$ = peak 2-second velocity at 10 m during record

$\hat{u}_h$ = peak 2-second velocity at the ridge height

z_o = roughness length

$\bar{\beta}$ = mean wind direction relative to true north

$\bar{\theta}$ = mean wind direction relative to the axis of the experimental building

σ_p = rms pressure over record length

WIND LOADS ON LOW-RISE BUILDINGS - EFFECTS OF ROOF GEOMETRY

by K J Eaton, J R Mayne and N J Cook

1 INTRODUCTION

A previous paper[1] presents preliminary results from the measurement of wind pressures which have been made by the Building Research Establishment on low-rise buildings at Aylesbury. The motivation and objectives of the experiment were explained in the introduction to that paper, and the site, installation, recording equipment and analysis procedures were also described in some detail.

This present paper therefore begins, in Section 2, with a short summary of the installation, given for the sake of clarity, but the earlier paper should be consulted for more detail. Section 3 presents full-scale measurements taken from new records which were obtained in the later stages of the project. These results follow on from the earlier ones, and give pressures recorded on the walls and on the roof of the experimental building for an extended range of roof pitches and for some different wind directions.

The data also include pressures measured on the upper surface of an overhang which was added to the western eaves of the building towards the end of the project.

Subsequent sections present a comparison of some of the full-scale results with measurements made in the BRE boundary layer wind tunnel and with the present UK wind-loading code[2].

The high values of peak-factor which were recorded in the earlier paper are also subjected to further analysis.

2 SITE AND INSTALLATION

A detailed description of the site, the experimental building, the pressure transducers, the data acquisition system and the analysis has already been given[1]. A brief description only will be given here. The site, which was situated on the south-west outskirts of Aylesbury, comprised a local authority estate of two-storey houses in several parallel terraces (Figure 1). A long fetch of open country extended to the south-west, whilst the terrain in the opposite direction was largely urban.

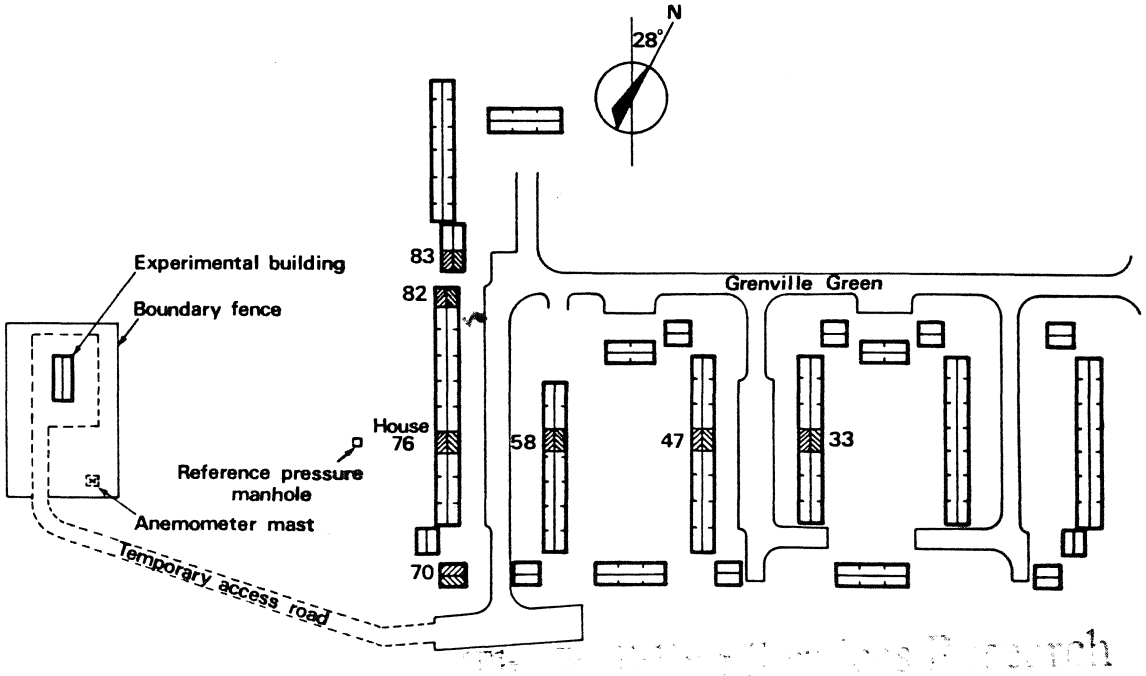

Figure 1 Plan of Aylesbury site

To the west of the estate on adjoining open ground, an experimental building was erected, also shown in Figure 1. The pitch of the roof was variable between 5° and 45°. In the latter stages of the project, an overhang of 0.7 m was added to the western eaves of the building extending along the middle third of the face, the length of this overhang being 4.5 m. One pressure transducer was fitted to the middle of the upper face of this overhang and another was fitted underneath. The inclination of the overhang followed the roof pitch.

Figure 2 shows the positions of the transducers on the experimental building and on the seven instrumented houses in the estate, and Figure 3 shows the experimental building with the overhang installed and the roof at 45°.

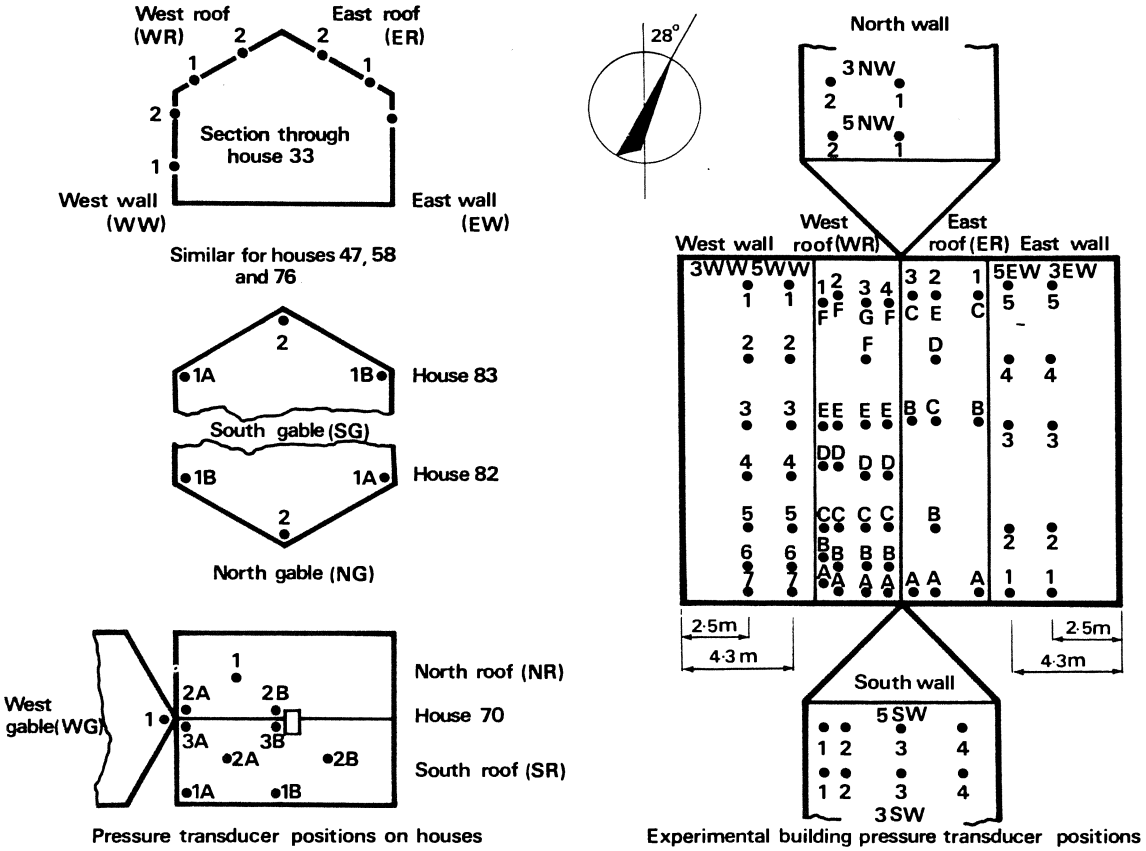

Figure 2 Position of pressure transducers on houses in the estate and on the experimental building

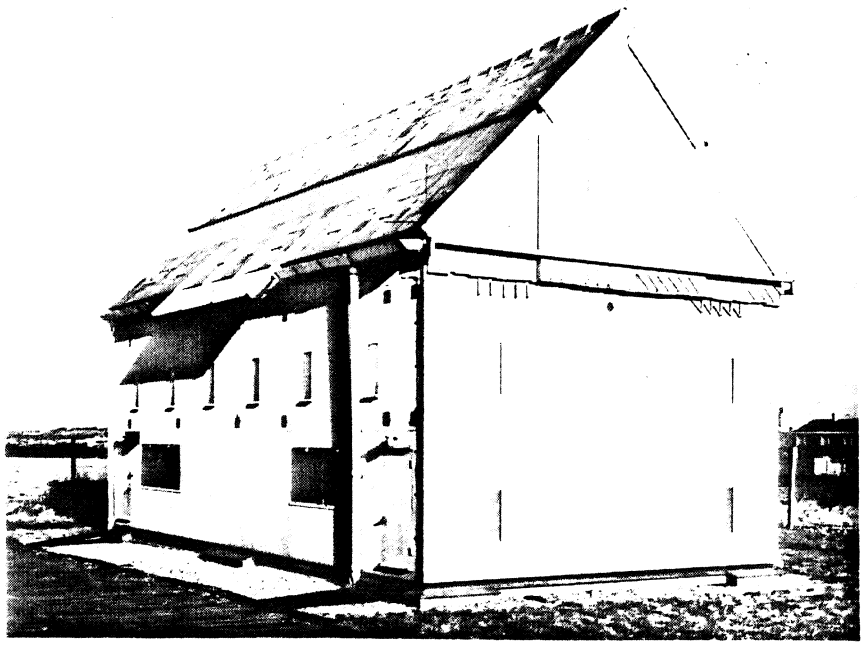

Figure 3 Experimental building with 45° roof pitch, showing eaves overhang

The transducers, both in the houses on the estate and in the experimental building, were vented to a common reference pressure close to static pressure, obtained from a manhole in the field between the experimental building and the estate, the position of which is marked in Figure 1. Unjointed lengths of cable connected each transducer to a recording room inside the experimental building. Records were obtained in analogue form on magnetic tape and were subsequently digitised at 32 Hz real-time.

Wind speeds were recorded by three cup-anemometers mounted on a mast near to the experimental building at heights of 3, 5 and 10 m, and direction was recorded at 10 m only. The mast was placed about 30 m from the experimental building in a position where it was unobstructed by the building for the wind directions most frequently occurring. The signals from these instruments were also recorded on magnetic tape concurrently with measurements of pressure. The frequency response of the anemometers was however limited to 0.5 Hz owing to the inertia of the cups.

3 FULL-SCALE RESULTS

The results presented in Figures 4 to 8 are from two records obtained in the early part of 1974. Details of these records are given in Table 1. Tables 2-12 give the full data for these records in numerical form. Record A35 covers four roof pitches from $22\frac{1}{2}^{o}$ downwards with the wind blowing in a direction not represented in previous records. A38 covers seven roof pitches over the full range of operation of the roof, but with the same wind direction as records A11 and A12 reported previously[1]. A38F (45^{o}) and A38G ($22\frac{1}{2}^{o}$) are however in slightly different wind conditions, as the wind unfortunately veered and decreased during these last two sections of the recording.

Table 1 Details of records taken at Aylesbury

Record no	Date	Time GMT	$\bar{\beta}$	$\bar{\theta}$	$\bar{u}_{10}$ (m/s)	$\hat{u}_{10}$ (m/s)	Roof pitch of experimental building
A35F	27.1.74	23.16	180^{o}	208^{o}	12.4	18.9	22.5^{o}
A35G	27.1.74	23.41	180^{o}	208^{o}	11.2	18.8	15.0^{o}
A35H	28.1.74	00.04	180^{o}	208^{o}	11.1	17.0	10.0^{o}
A35J	28.1.74	00.26	180^{o}	208^{o}	10.5	14.0	5.0^{o}
A38A	10.2.74	11.49	205^{o}	233^{o}	12.4	21.1	15.0^{o}
A38B	10.2.74	12.16	205^{o}	233^{o}	11.3	20.4	10.0^{o}
A38C	10.2.74	12.40	205^{o}	233^{o}	11.1	18.4	5.0^{o}
A38D	10.2.74	13.12	205^{o}	233^{o}	11.5	19.9	27.5^{o}
A38E	10.2.74	13.38	205^{o}	233^{o}	11.4	18.3	35.0^{o}
A38F	10.2.74	14.08	210^{o}	238^{o}	10.2	18.8	45.0^{o}
A38G	10.2.74	14.48	220^{o}	248^{o}	8.3	14.9	22.5^{o}

In every case mean coefficients are based upon the mean velocity measured on the nearby mast at a height of 10 m over the total length of the record (1024 seconds). Peak coefficients are based upon the 10 m 2-second velocity, but the corresponding pressures relate to extremes of 1/32-second duration. Only in Section 6 is this procedure altered, where, for Code comparisons, velocities are used for heights appropriate to those used in design, ie the ridge height of the building.

Figure 4 (a-g) shows mean pressure coefficients for the roof of the experimental building over the full range of roof pitches from 5^{o} to 45^{o} with a skew wind blowing mainly at 37^{o} to the normal to the major face of the building. Figure 5 (a-h) shows the corresponding peak pressure coefficients, positive and negative limits being given for the 35^{o} roof pitch where the mean is near zero over most of the windward roof (Figure 5 f and g). At 45^{o} (Figure 5 h) only positive limits are given, whilst at angles below 35^{o} (Figure 5 a-e) only negative limits are given.

The figures show some similarities to those presented for A11 and A12[1], notably the position of the high suction region on the windward edge of the roof a short distance from the corner (transducers WR1B and WR1C). For the present record however, the mean coefficients are rather lower whilst the peak coefficients are considerably higher. The mean velocity in the present records (A38) is however higher than previously (A11 and A12), but as the direction and the turbulence intensity are similar, this difference between the two sets of data is unexplained.

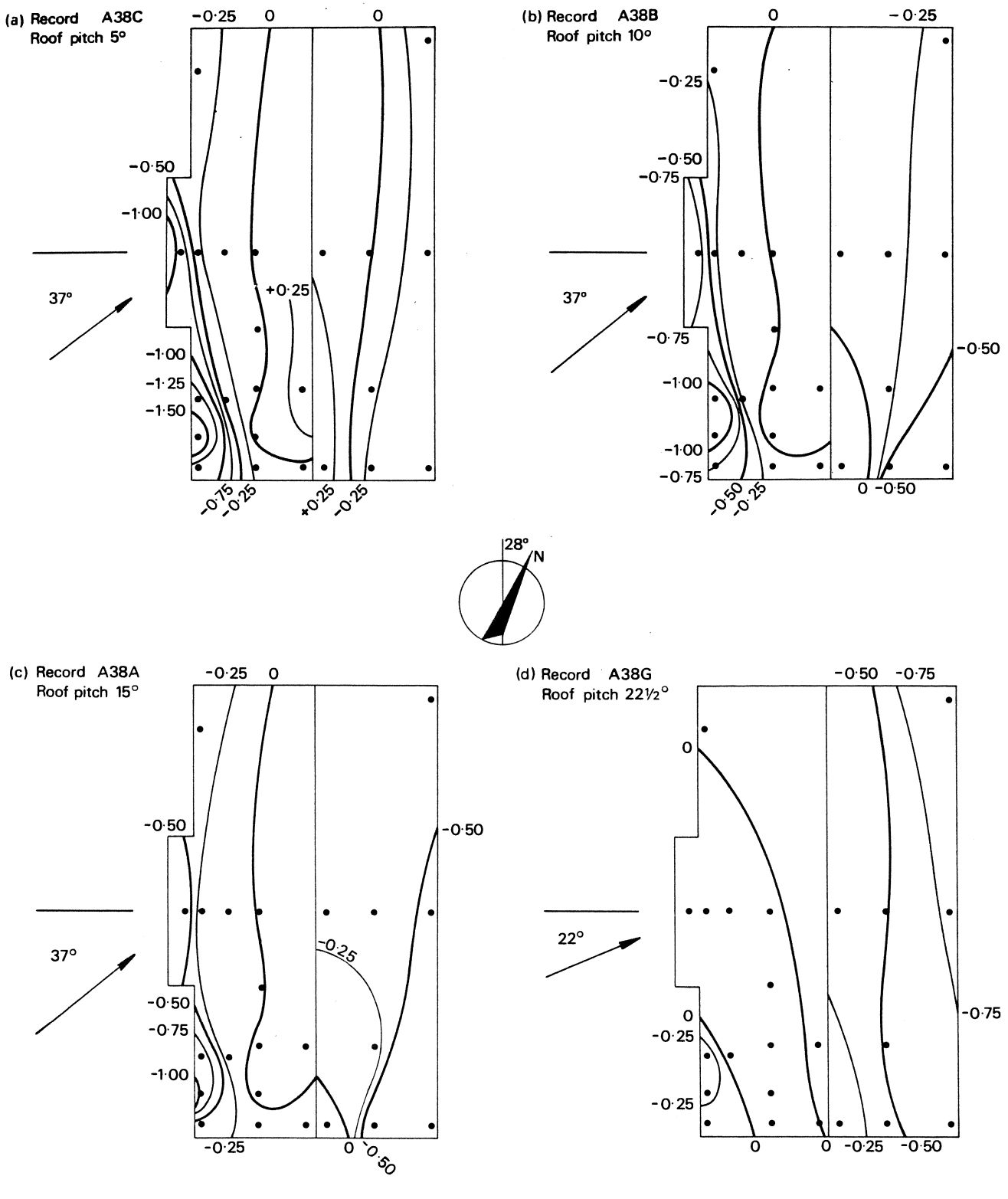

Figure 4 Mean pressure coefficients on roof of experimental building

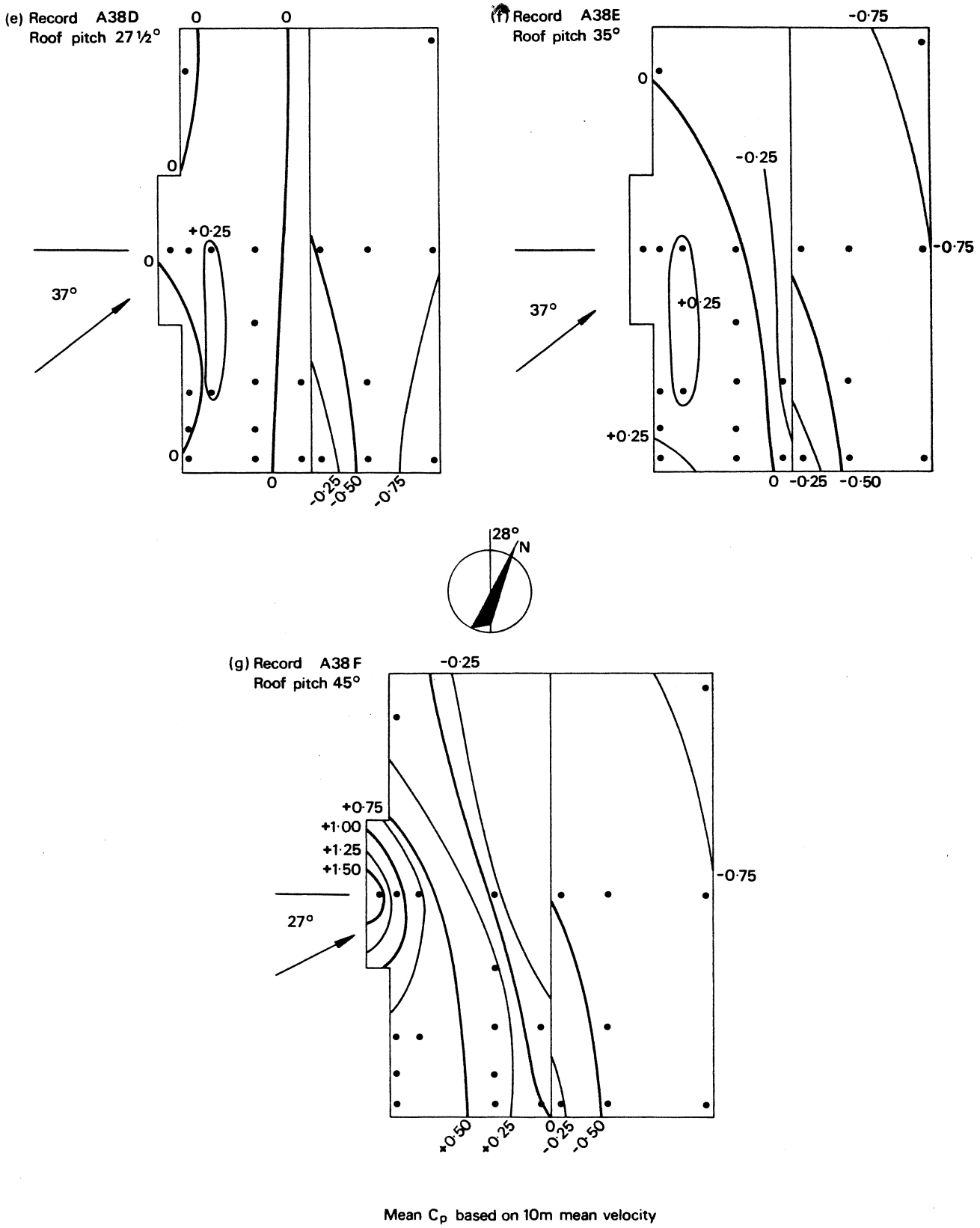

Figure 4 (Continued) Mean pressure coefficients on roof of experimental building

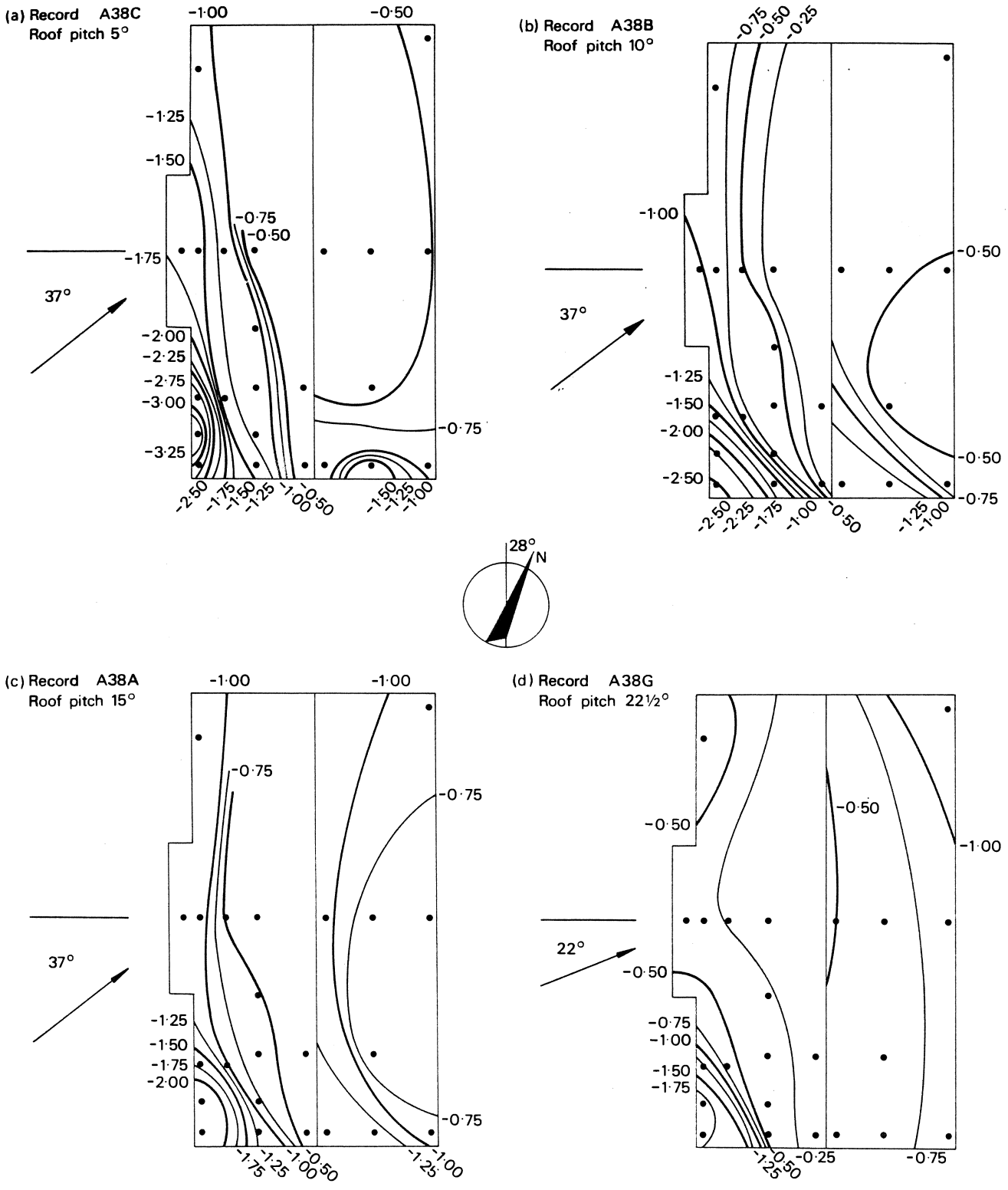

Figure 5 Peak pressure coefficients on roof of experimental building

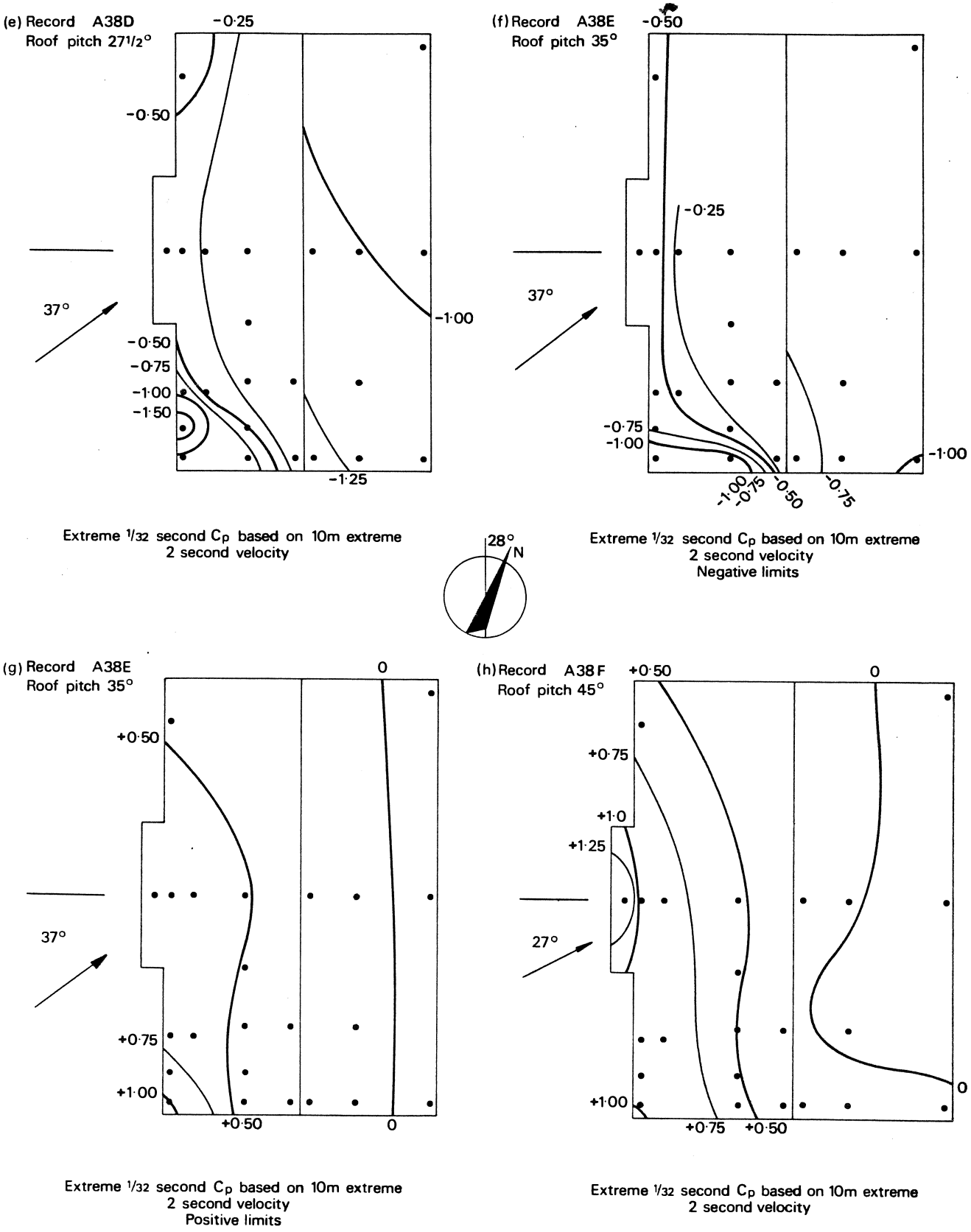

Figure 5 (Continued) Peak pressure coefficients on roof of experimental building

A marked trend is evident towards more negative roof pressures and towards high local suctions on the windward roof as the roof pitch becomes lower. The severest loadings occurred at the lowest pitch (5°). This trend is shown in Figure 6, where coefficients from transducer WR1B in the local high suction area have been plotted directly against roof pitch. The mean, the positive and negative extremes and the positive and negative 0.05 per cent quantiles are shown. Other transducers on the windward roof show the same trend to a lesser degree. Pressures on the leeward roof are more erratic, and these are shown by a shaded band which tends in the opposite direction, the most negative pressures occurring at the highest roof pitch, ie when that part of the roof is fully immersed in the wake.

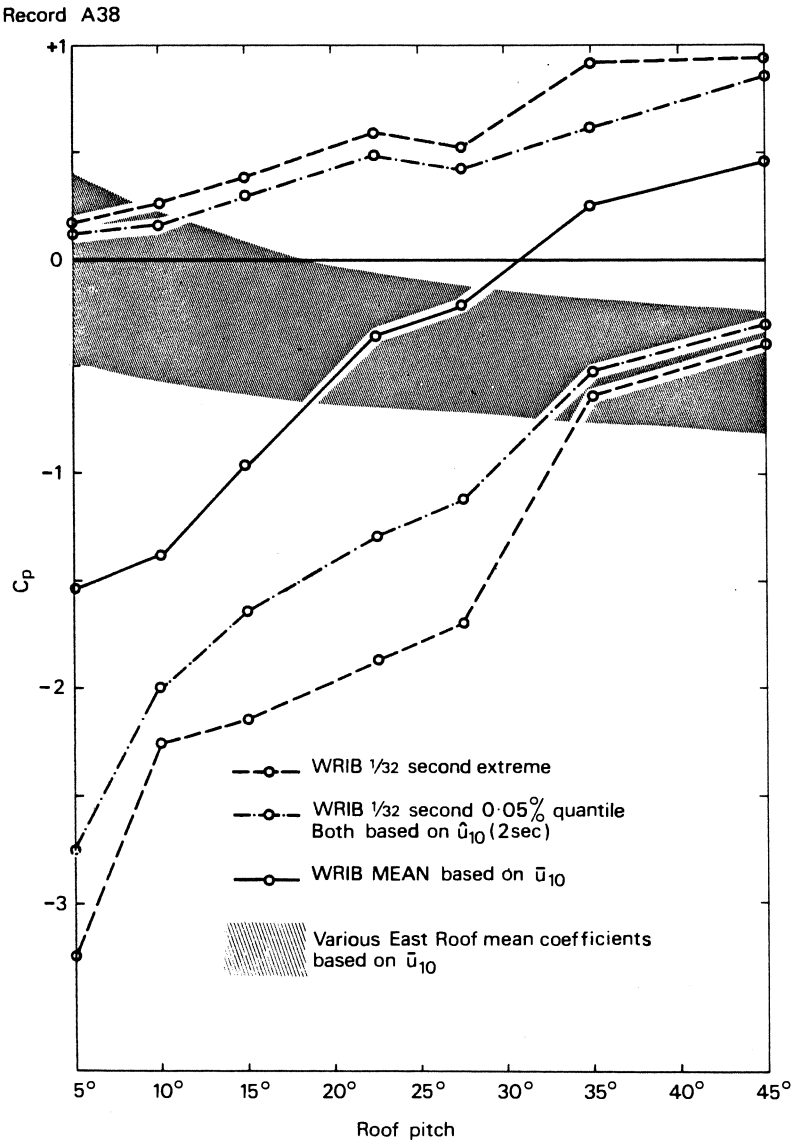

Figure 6 Variation of roof pressures with roof pitch

Figures 7 (a-d) and 8 (a-d) show similar data to Figures 4 and 5 for another skew wind direction more nearly end-on to the building (62° to the major face). The range of roof pitches is 5° to $22\frac{1}{2}$°. A local high pressure region, corresponding to that found for record A38, occurs along the windward edge of the roof, in this case the south edge, again with the maximum value away from the corner and centred around transducer WR3A. For this wind direction, the roof overhang also receives a high uplift, particularly severe at 5° pitch. Again the loads become more negative and more severe with decrease of roof pitch.

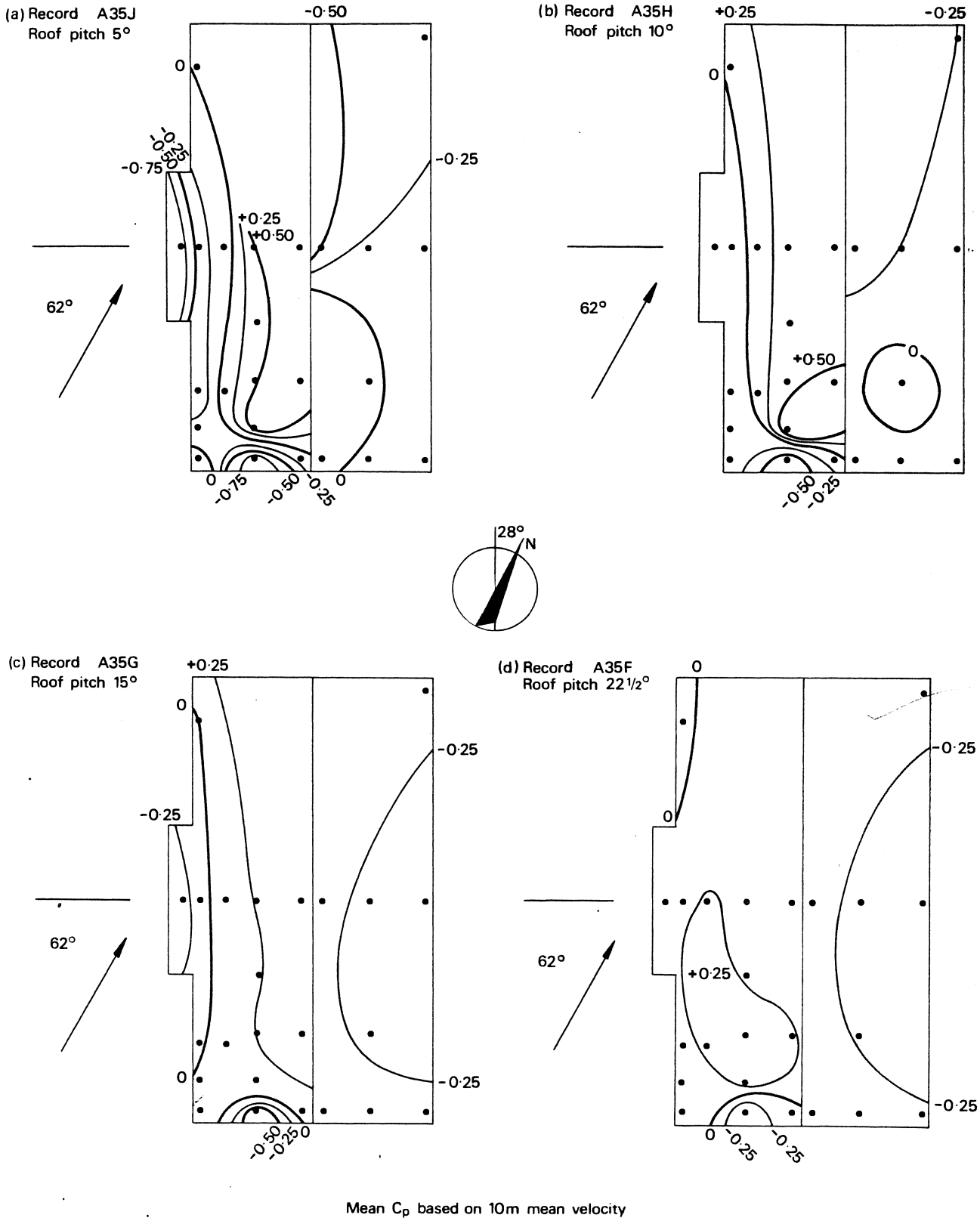

Figure 7 Mean pressure coefficients on roof of experimental building

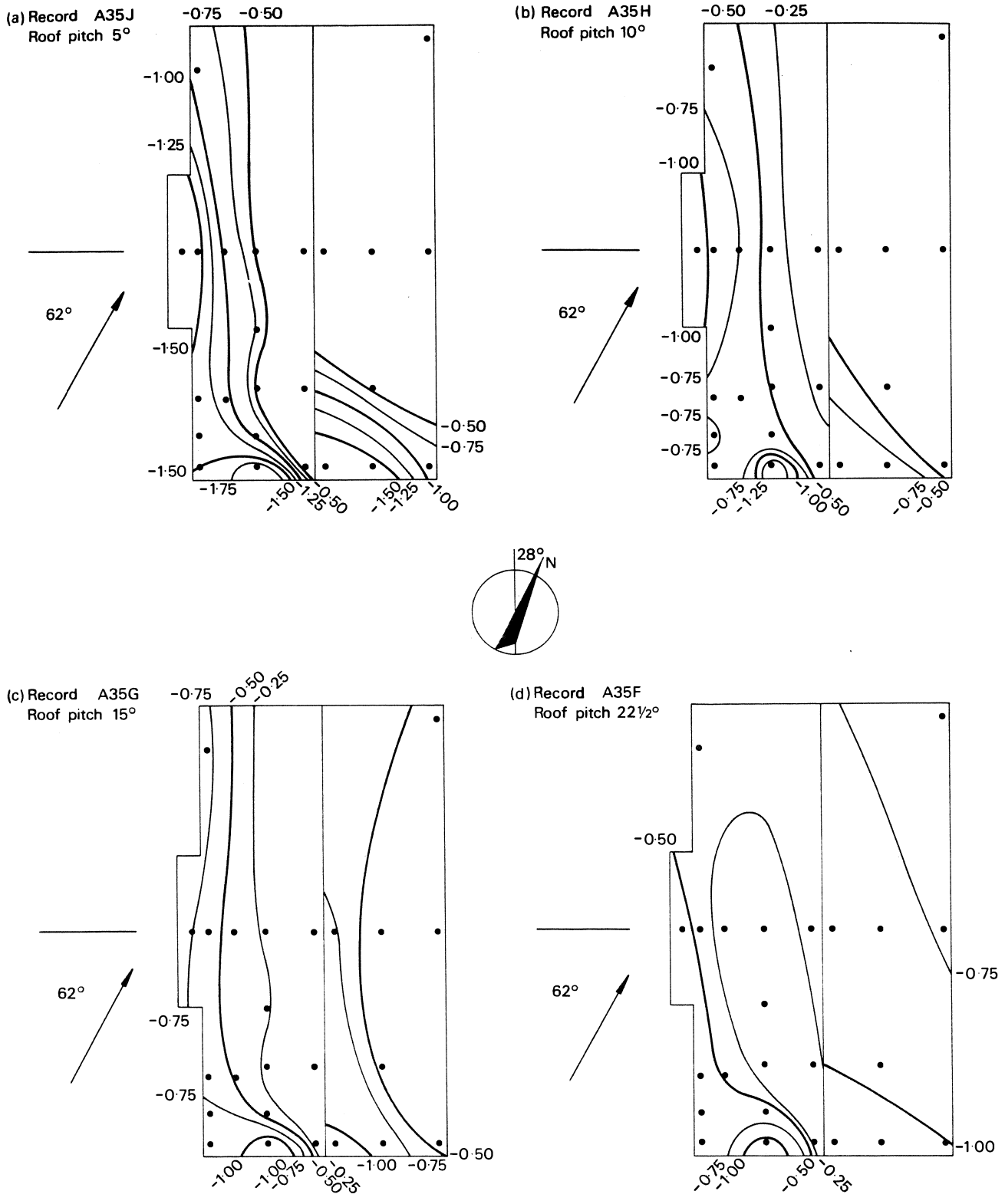

Figure 8 Peak pressure coefficients on roof of experimental building

4 WIND TUNNEL COMPARISON

It was intended to reproduce the full-scale experiments A35 and A38 at model scale in the new BRE boundary layer wind tunnel and to investigate some intermediate wind directions and roof pitches. Delays in acquisition of data processing hardware left insufficient time to attempt the complete model tests before the time of writing.

Some results from preliminary tests on a 1/50-scale model of the experimental building at $22\frac{1}{2}^{o}$ roof pitch have been included for comparison with full-scale results. An adequate simulation of the turbulent atmospheric boundary layer appropriate to the Aylesbury site is not possible at 1/50-scale in the boundary layer wind tunnel at this time. Only the mean velocity profile was correctly simulated by matching the roughness parameter, z_o; the turbulence characteristics were deficient in integral scale and intensity. Therefore the measured peak pressures have not been presented since they are not considered representative of the full-scale situation. A new model at 1/100-scale with roof pitches of 5^{o}, 10^{o}, 15^{o} and $22\frac{1}{2}^{o}$ is presently under construction, and will be tested in adequately simulated turbulence and shear. The results of these tests will be presented in a future paper.

In this paper comparison between the model and full scale is confined to mean pressure coefficients. Over periods of time equivalent to 1000 seconds at full scale, mean pressures showed reasonable agreement for the walls, but not such good agreement for the roof. It was however possible to reproduce the high-pressure zone recorded at full scale in record A35 near transducer WR3A and to find the wind direction for which these pressures were a maximum. This was at 74^{o} to the normal to the major face. The corresponding area of high local suction for record A38 could not be studied because the 1/50-scale model had no roofs at the lower pitches.

Figure 9 (a and b) shows a comparison between mean wall pressures on the experimental building from record A35 and for the same wind direction in the wind tunnel. Both sets of coefficients are based on the mean velocity at 10 m. The results show very good agreement except for the 4.3 m level on the west face for which the full-scale result shows almost twice the pressure shown in the wind tunnel. Several sets of wall pressure comparisons for the wind blowing at other directions more nearly normal to the major face showed the same discrepancy.

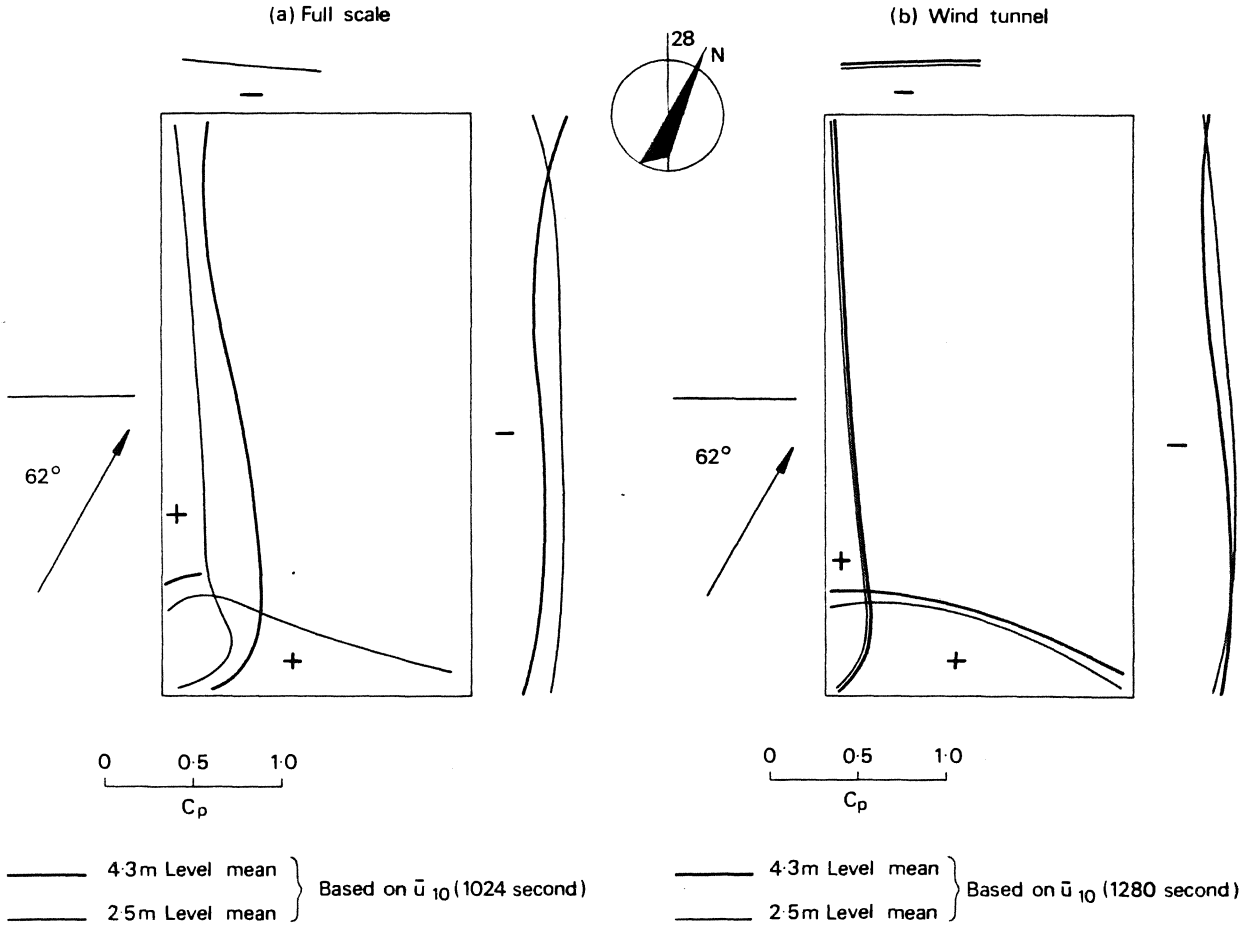

Figure 9 Mean wall pressure coefficients on experimental building: comparison of full-scale and wind-tunnel results

5 PEAK-FACTORS

A parameter which, it has been suggested[3], may offer a useful approach to the design of cladding is the peak-factor, g, defined by:

$$g = (\hat{p}_t - \bar{p})/\sigma_p \qquad \ldots\ldots\ldots\ldots (1)$$

The value of this factor will depend upon the particular point on a building at which the pressure is measured. However the peak-factor is also affected by analysis and measurement techniques, since the value clearly depends, for example, upon the effective period over which the maximum pressure is measured. It is this latter type of effect which is discussed in the following paragraphs, since unfortunately analysis and measurement techniques differ so greatly between different projects, and these effects often mask aerodynamic differences.

The measurements made at Aylesbury make it possible to show how important these effects can be. Owing to the inherently statistical nature of the extreme pressures which are recorded, the data recorded at Aylesbury were analysed by computing pressure values corresponding to various quantiles in the tail of the probability distribution function. These points were the 50, 10, 1, 0.1, 0.05 and 0.01 per cent levels. Furthermore the calculations were repeated for averaging periods ranging from 1/32 second up to 32 seconds, in each case covering the whole length of the record, which was 1024 seconds. This was done in the following way.

The distribution of the full set of 32 768 data points (every 1/32 second for the whole length of the record) was analysed, and the required quantile levels were determined. The data were then averaged in consecutive non-overlapping pairs to obtain the 1/16-second data, thereby halving the number of samples, and the quantile levels were again determined. The process was repeated until the data corresponded to 32-second averaging periods. For the longest averaging periods the more extreme quantiles could not be calculated, because the data sample became too small.

Figure 10 is a typical contour plot produced from these calculations, showing how the peak-factor varies as a function of both quantile level and averaging period on the west wall. The plot shows

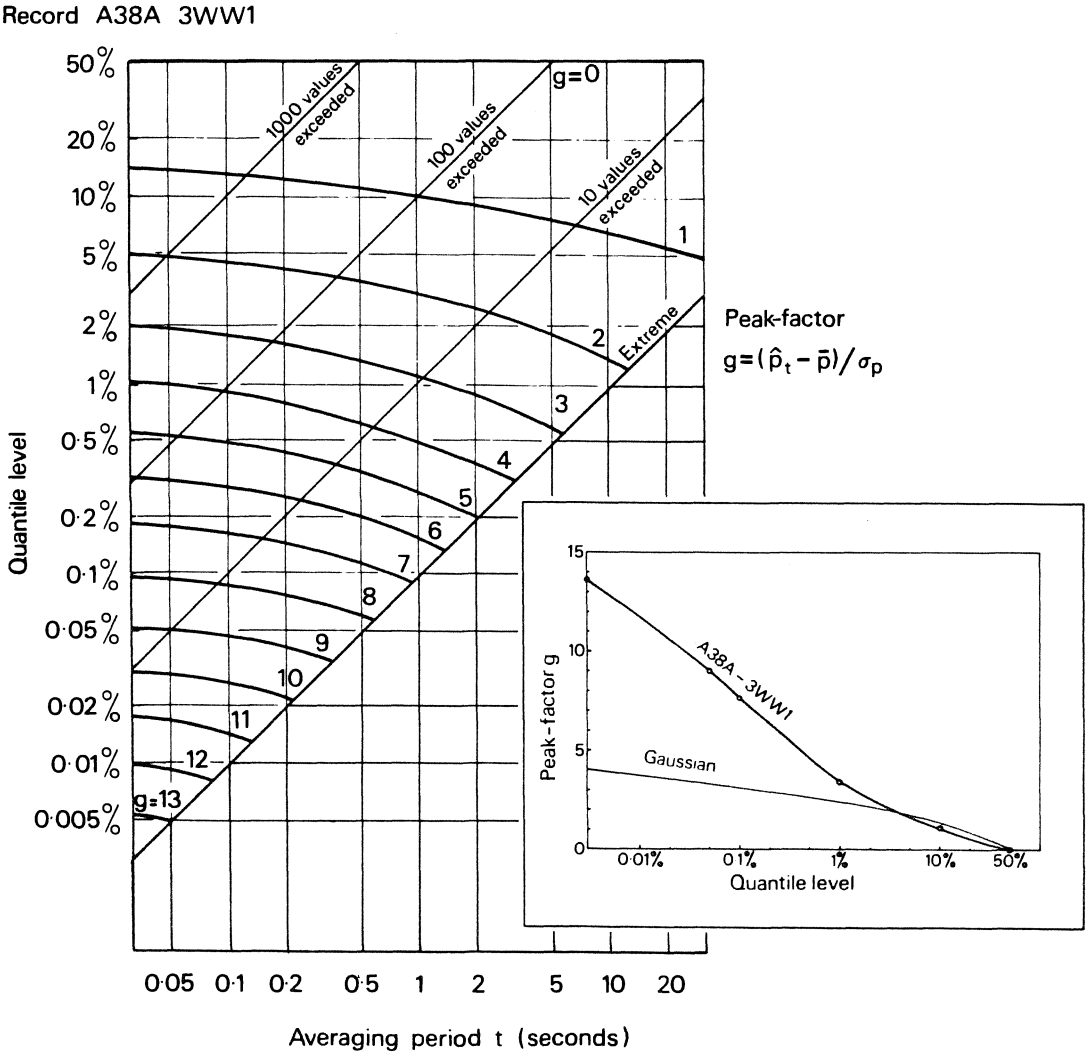

Figure 10 Contours of peak-factor as a function of quantile level and averaging period

clearly that the highest peak-factors recorded are confined to a very small area of the averaging period - quantile domain.

In any experiment, the peak-factors measured are thus critically dependent upon the measurement and analysis procedures adopted. For example g depends upon:

(i) the sample size (ie the number of data points collected) which will determine the quantile level which can be included

(ii) the response of the transducer, and

(iii) the digitising rate, both of which will determine the minimum duration which is recorded.

Many values of peak-factor recorded at Aylesbury [1] are very high when compared with values reported elsewhere [3,4] and these differences are almost certainly due largely to measurement and analysis techniques. All the values given for the Aylesbury experiment have referred to 1/32-second extreme values, equivalent to the highest value of 13.7 shown in Figure 10. This figure also shows that, for this particular record, the value of peak-factor for a 1-second extreme was between 6 and 7, and that for a 1/32-second 1 per cent quantile, was 4.

It can also be seen how far the pressure distribution departs from Gaussian, especially in the tail of the distribution where the extreme values occur, a fact which is well known but frequently overlooked. In the inset of Figure 10, a section along the vertical 1/32-second axis of the contour plot is compared with the peak-factors which would be obtained if the distribution were Gaussian. For the 0.01 per cent quantile, the departure from the mean in a Gaussian distribution is about 4σ, ie $g = 4$. The measurements made at Aylesbury, however, invariably give values of g in excess of 4 and in many cases in excess of 10. The distribution appears much more nearly Gaussian if comparisons are made of longer averaging periods or less far into the tail of the distribution, and the results of many full-scale and wind tunnel experiments are confined to the near Gaussian region either by limitations of the response of the measurement equipment, or by choice in order to produce statistically stationary data.

6 RELATION TO DESIGN

Results from a full-scale project of this type are useful for comparisons with wind-loading codes of practice. This is particularly so in the case of the data obtained from the variable pitch roof of the experimental building because most codes present variations of pressure coefficients with roof pitch changes.

As indicated in Section 3, pressure coefficients in codes of pratice are usually based on the wind speed at the height of the top of the building. In the present case, this was the ridge of the experimental building, and it varied from 5.7 m at 5° pitch to 8.8 m at 45° pitch. In this section the appropriate velocity has been determined by interpolation between the data from the 3 m, 5 m and 10 m anemometers.

The United Kingdom Code of Practice [2], CP3:Chapter V:Part 2:1972, presents average pressure coefficients (intended for use with a 3-second dynamic pressure) for different areas of roofs, for roofs of various pitch, and for buildings of different height ratios. The experimental building at Aylesbury was a 'medium' height building as defined by the Code. With the wind blowing perpendicular to the ridge, as the roof pitch varies from 5° to 45°, the average value of pressure coefficient over the windward slope varies in the Code from -1.1 to +0.2. A direct comparison with the measured data is not attempted here because, as already stated, there appears to be a discrepancy between A11, A12 and A38. However, allowing for the lower velocities at the ridge height as compared with a height of 10 m, the measured pressure coefficients do appear to be in reasonable accord with the Code. Here it must be remembered that the experimental building is an isolated structure in a field, and that conditions in an urban area will be very different, as is shown by comparing the pressures recorded on the estate with those on the experimental building [1].

The Code data also include local pressure coefficients (that are used for cladding design) all round the edges of the roof (eaves, verges and ridge). These are very much higher than the average values, particularly at the lower roof pitches, and this variation in the Code can be seen in Figure 11. Also plotted in this figure is an 'envelope' or range of local C_p values at various positions around the edge of the roof for the different roof pitches. These measured values are in fact 1/32-second extreme values (based on $\hat{u}_h$) and are directly comparable with the Code. From this it can be seen that parts of the perimeter of the roof are underdesigned and this clearly results in much of the wind damage that occurs to roofing [5,6].

When the further wind tunnel tests mentioned in Section 4 have been carried out, a considerable amount of interpolation and extrapolation to other roof pitches will be possible. It should also be

possible in the near future to determine the effects of permeability on the internal pressure of the experimental building, and also to determine the effects of variations in the layout and density of the estate of houses on the external pressure coefficients. These parts of the project will all have a considerable bearing on the design of low-rise structures.

7 CONCLUDING REMARKS

A pattern is beginning to emerge from the studies of variations of C_p with roof pitch and wind direction. Suction loads on roofs become more severe with decreasing roof pitch. This increase of loading continues down to 5^o, although the UK Code [2] allows for a maximum load at 10^o pitch. Unfortunately, no data are available for 0^o, but it is proposed to obtain this in further wind tunnel tests.

Mean pressures are useful for comparisons with measurements made in the wind tunnel. However they have no counterpart in the Code which requires maxima only. Even the overall loads are assessed by maxima, although the averaging period used may be quite long, eg 5 or 15 seconds.

In general it is the peak values, $C_{\hat{p}}$, that are most interesting and useful for design comparisons, and in the present context of small low-rise buildings it is the very short duration loadings which are important.

The full-scale and wind tunnel results clearly show the areas of high suction on the roof with a skew wind, these being in a localised zone a short distance from the windward corner. The magnitudes of these local coefficients are of the order of -3.0 (when based on $\hat{u}_{10}$) at 5^o pitch; this is equivalent to about -3.8 when based on $\hat{u}_h$, where h is the ridge height.

Extremes of 1/32-second duration, when plotted as in Figure 11, cover a band which encloses the values used in the Code. Since the local coefficients given in the Code are compromises intentionally set below the absolute maxima (in order to compensate for the spatial distribution of loadings and to allow for load sharing between various parts of the structure), this is to be expected. For example local coefficients are applied over a band around the edge of a roof of dimension equal to 0.15 times the width of the building (about 1 m in the case of the Aylesbury building). The coefficient of -2.0 which the Code applies should be compared with the transient localised pressure zone of -3.8 referred to above. Comparisons such as this suggest that the actual maxima are often too much in excess of the Code requirements in certain cases (eg the edges of roofs) and this view is confirmed by studies of damage [5,6]. Consideration should therefore be given to increasing the Code values.

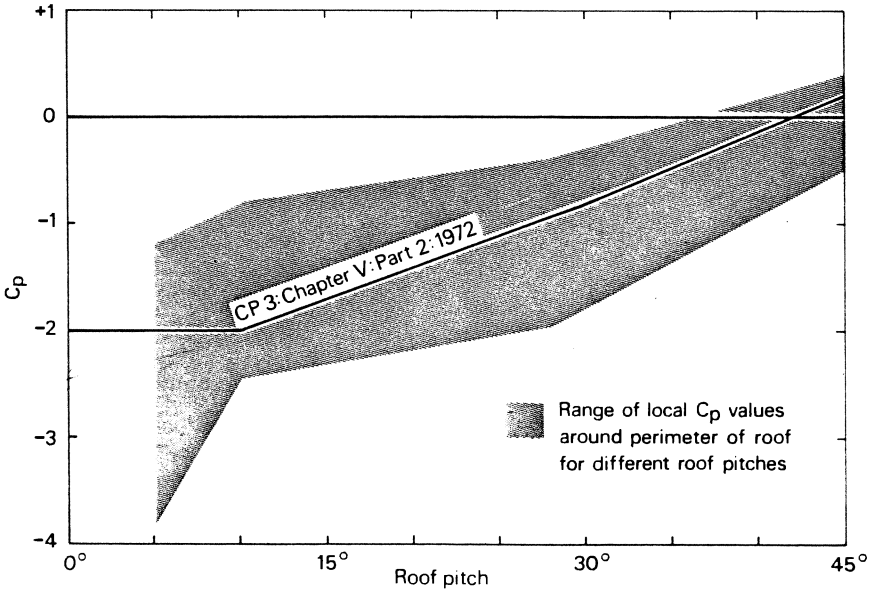

Figure 11 Comparison of measured roof pressures with Code requirements

The values of peak-factors recorded at Aylesbury emphasise the non-Gaussian distribution of the pressure fluctuations and the high population of the tails of the distributions. Caution is necessary in the interpretation of results and in comparisons between experiments because instrument response and methods of data collection and analysis have a great effect on recorded extremes.

A new theoretical model which is a better fit to the extreme value distribution is required to replace the Gaussian model. Other distributions have been used for this purpose before; the authors are considering using an approach based on the Weibull distribution.

8 CONFERENCE PRESENTATION

This section gives additional material presented at the Conference.

The high peak-factors such as those shown in Figure 10, are not due to faulty data (eg 'drop-outs' on the magnetic tape). The effect of a 'drop-out' is shown in Figure 12, and it results in a 'pyramid' on the contour plot which is easily detected.

The high peak-factors recorded at Aylesbury result entirely from the intermittent nature of the flow and turbulence causing the local pressure fluctuations. Such intermittency has been reported by other workers [7], and is illustrated in Figure 13.

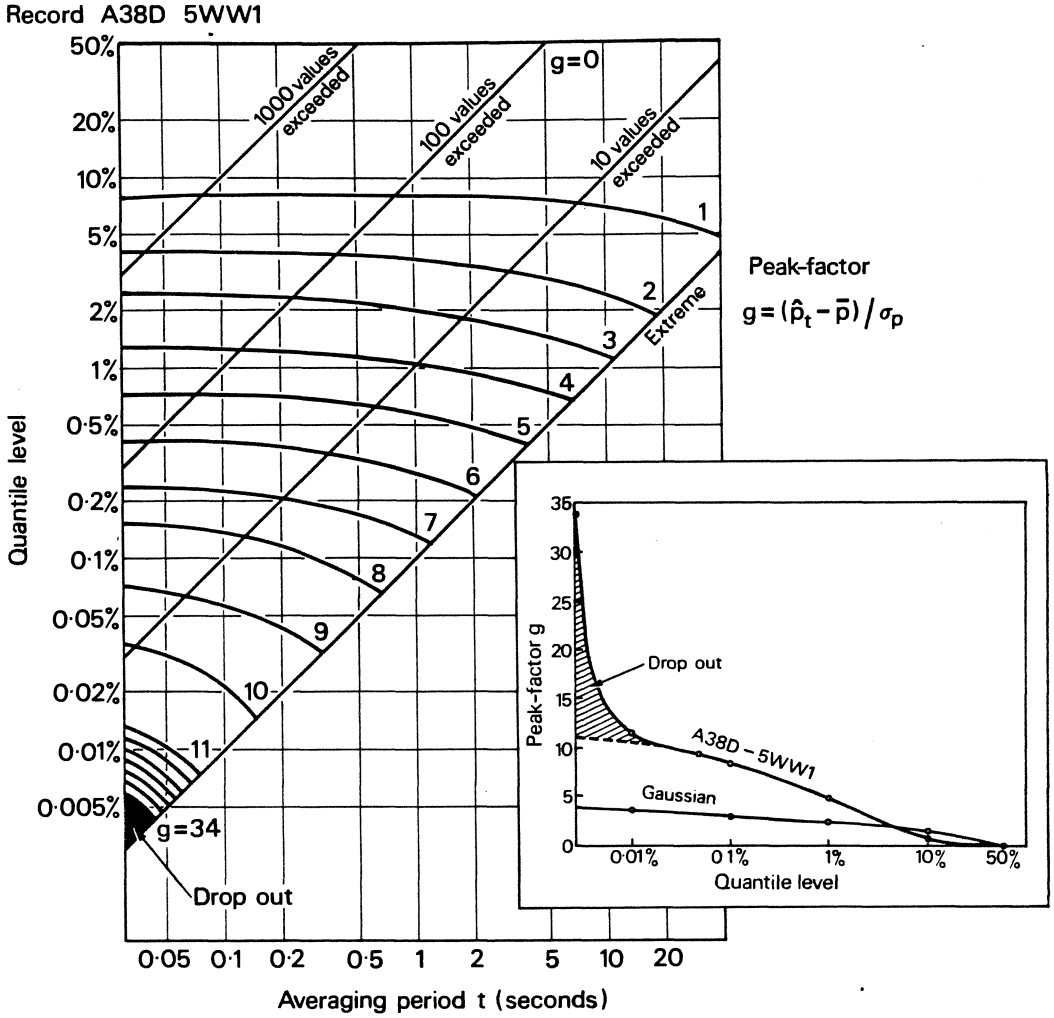

Figure 12 Contours of peak-factor as a function of quantile level and averaging period showing example of drop-out

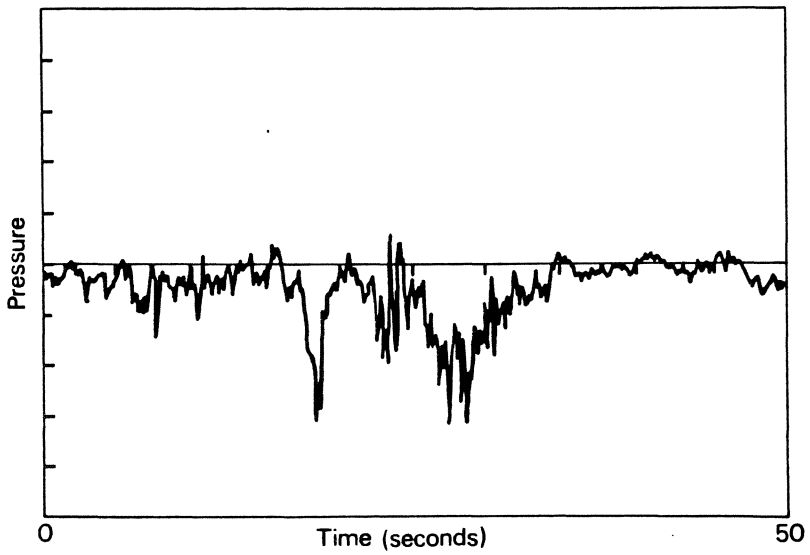

Figure 13 Typical variation of pressure with time showing intermittent bursts of turbulence

Equation (1) may be re-written as

$$\hat{p} = \bar{p} + g\sigma_p \quad \ldots\ldots\ldots\ldots (2)$$

In this form the peak loading is clearly seen to be divided into two parts, namely $\bar{p}$, which is effectively a static loading, and $g\sigma_p$, which is the short-term dynamic component of loading. The severity of the dynamic load is determined, not by g alone, but by the product $g\sigma_p$. In many cases high values of g are associated with low values of σ_p, so that the peak loading is not as great as might be inferred from consideration of the peak-factor values only. However, this is not always the case; the relative values of g and σ_p vary over different parts of the structure and Figure 14 shows this effect. The grids of hyperbolae represent constant values of $g\sigma_p$ in coefficient form ($g C_{\sigma_p}$). Figure 14a shows data from record A38C (5° roof pitch) plotted for the west wall only. The points fall in a fairly well defined area on the graph. Similarly, Figures 14 b–e show data from the same record for other parts of the building, namely east wall,

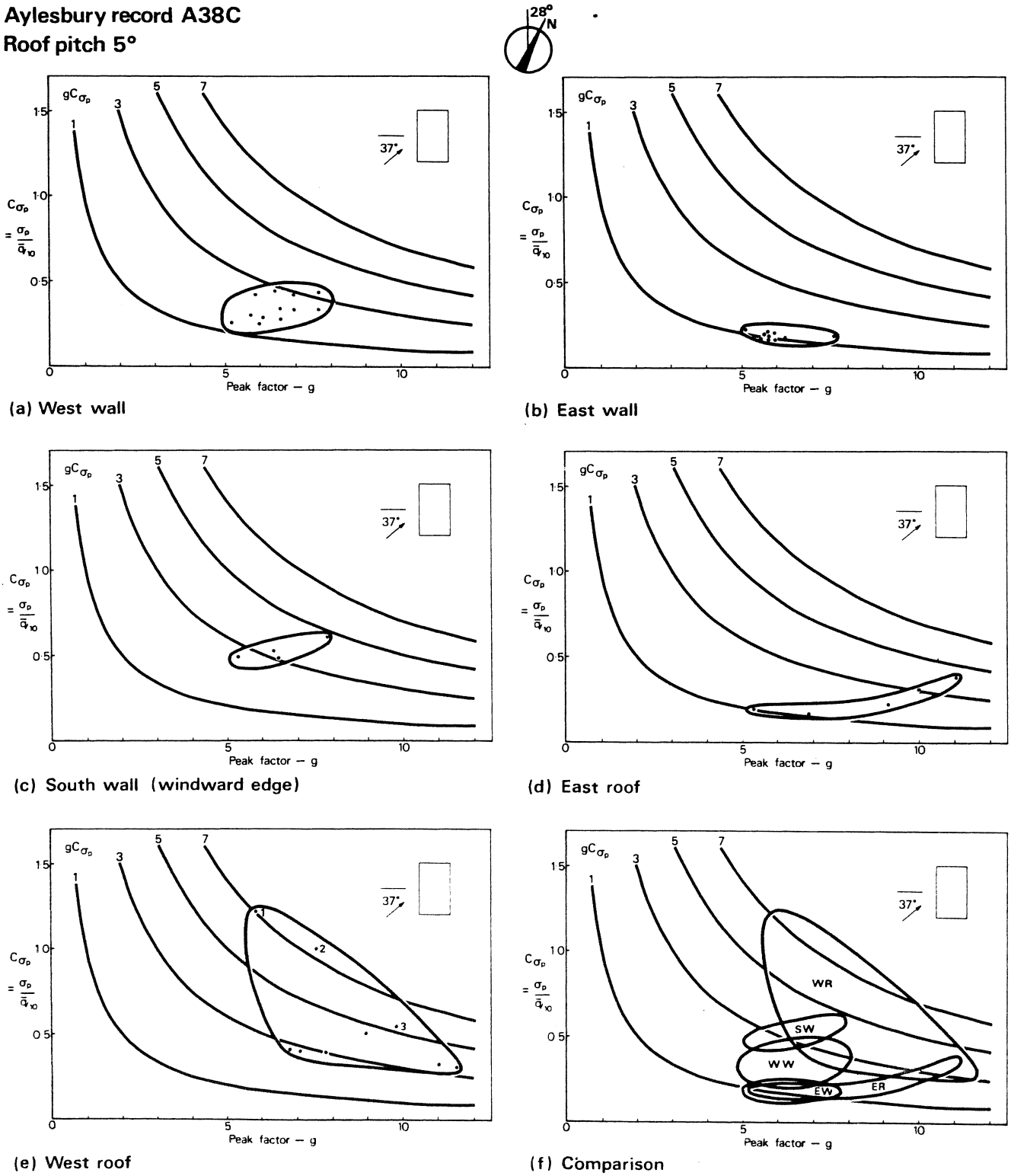

Figure 14 Showing dynamic pressures in coefficient form for various parts of the experimental building

south wall (windward edge), east roof and west roof. The points are most widely scattered in the case of the west roof, because of the different types of flow (eg separated and attached) occurring over the windward half of the roof. The points in Figure 14e marked 1, 2 and 3 are from transducer positions WR1A, WR1B and WR1C respectively, and these positions near the windward corner of the roof show the highest peak loading on the whole building, but with very different proportions of g and σ_p.

The interpretation of these results is continuing and will be the subject of a further paper.

9 ACKNOWLEDGEMENTS

The authors wish to thank Aylesbury Vale District Council and their tenants for their co-operation at all stages of this experiment. They also gratefully acknowledge the assistance provided by the Environmental Sciences Research Unit at Cranfield and all the staff of the Wind Loading Section at the Building Research Station.

10 REFERENCES

1 **Eaton, K J** and **Mayne, J R.** The measurement of wind pressures on two-storey houses at Aylesbury. Symposium on Full-Scale Measurements of Wind Effects on Tall Buildings and Other Structures, University of Western Ontario, London, Ontario, June 1974. (Also BRE Current Paper CP 70/74.)

2 **British Standards Institution.** Code of Practice CP 3:Chapter V:Part 2:1972: Wind loads. BSI, London.

3 **Dalgliesh, W A.** Statistical treatment of peak gusts on cladding. Journal of the Structural Division, ASCE, Vol 97, No ST9, September 1971, pp 2173-2187.

4 **Newberry, C W, Eaton, K J** and **Mayne, J R.** Wind loading on tall buildings - further results from Royex House. Industrial Aerodynamics Abstracts, Vol 4, No 4, July-August 1973. (Also BRE Current Paper CP 29/73.)

5 **Menzies, J B.** Wind damage to buildings in the United Kingdom, 1962-1969. Building, Vol 221, No 6693, 27 August 1971, pp 67-76. (Also BRS Current Paper CP 35/71.)

6 **Eaton, K J** and **Menzies, J B.** Roofs, roofing and the wind. Proceedings International Symposium on Roofs and Roofing, Brighton, September 1974, Vol 1, Paper 6. (Also BRE Current Paper CP 75/74.)

7 **Melbourne, W H.** Cross-wind response of structures to wind action. Proceedings 4th International Conference on Wind Effects on Buildings and Structures, London, September 1975. Cambridge University Press. (In Press.)

Table 2 Record A35F

	$\bar{p}$ (Nm^{-2})	σ_p (Nm^{-2})	p_{max} (Nm^{-2})	p_{min} (Nm^{-2})	g (1/32 sec)	$C_{\bar{p}}$	$C_{\hat{p}}$ (2 sec)	$C_{\hat{p}}$ (1/32 sec)
3WW1	8	11	72	-63	6.5	0.08	0.17	0.33
3WW2	13	12	85	-36	6.0	0.14	0.24	0.39
3WW3	22	14	91	-28	4.9	0.23	0.33	0.42
3WW4	23	18	112	-43	4.9	0.25	0.42	0.52
3WW5	22	17	101	-70	5.4	0.23	0.39	0.46
3WW6	37	44	210	-212	5.7	0.39	0.76	-0.97
3WW7	11	41	159	-192	5.0	0.12	0.57	-0.88
5WW1	26	13	110	-7	6.5	0.27	0.31	0.50
5WW2	25	16	112	-10	5.4	0.26	0.37	0.51
5WW3	43	20	142	-9	4.9	0.45	0.57	0.65
5WW4	50	21	157	-8	5.1	0.52	0.64	0.72
5WW5	56	24	157	-36	4.2	0.59	0.67	0.72
5WW6	52	35	181	-89	4.0	0.55	0.74	0.83
5WW7	31	51	177	-191	4.4	0.32	0.78	-0.88
3EW1	-44	14	-8	-105	4.4	-0.46	-0.42	-0.48
3EW2	-47	14	-13	-116	4.9	-0.50	-0.45	-0.53
3EW3	-49	15	1	-127	5.2	-0.52	-0.46	-0.58
3EW4	-43	15	1	-122	5.3	-0.46	-0.43	-0.56
3EW5	-41	16	5	-131	5.6	-0.44	-0.43	-0.60
5EW1	-32	11	-1	-93	5.5	-0.34	-0.33	-0.42
5EW2	-38	12	-9	-96	4.8	-0.40	-0.38	-0.44
5EW3	-44	15	-5	-156	7.5	-0.46	-0.40	-0.71
5EW4	-35	15	1	-121	5.7	-0.37	-0.34	-0.55
5EW5	-36	17	9	-199	9.6	-0.38	-0.50	-0.91
3SW1	51	24	207	-127	7.4	0.54	0.56	0.95
3SW2	54	24	359	-117	12.7	0.57	0.63	1.65
3SW3	35	20	140	-43	5.2	0.37	0.44	0.64
3SW4	17	13	159	-37	10.9	0.18	0.26	0.73
5SW1	65	32	227	-143	6.5	0.69	0.80	1.04
5SW2	20	16	140	-8	7.5	0.21	0.40	0.64
3NW1	-26	9.4	-1	-75	5.2	-0.27	-0.27	-0.34
3NW2	-28	11	-2	-91	5.7	-0.30	-0.28	-0.42
INT	9	8.1	39	-27	4.4	0.10	0.11	0.18
OH-U	4	24	76	-141	6.0	0.04	-0.35	-0.65
OH-L	46	20	151	-6	5.2	0.49	0.58	0.69
WR1A	9	19	112	-119	6.7	0.10	0.29	-0.55
WR1B	16	17	104	-114	7.6	0.17	-0.31	-0.52
WR1C	19	18	85	-141	8.9	0.20	-0.30	-0.65
WR1E	-2	16	106	-100	6.7	-0.02	0.23	0.49
WR1F	-5	12	40	-90	7.1	-0.05	-0.17	-0.41
WR2C	26	12	80	-74	8.3	0.27	0.27	0.37
WR2E	15	10	67	-37	5.2	0.16	0.21	0.31
WR3A	-25	31	93	-247	7.2	-0.26	-0.44	-1.13
WR3B	30	26	138	-143	6.7	0.32	0.39	-0.66
WR3C	30	13	87	-13	4.4	0.32	0.30	0.40
WR3D	20	15	72	-40	4.0	0.21	0.26	0.33
WR3E	25	13	77	-25	4.0	0.26	0.26	0.35
WR4C	24	17	92	-53	4.5	0.25	0.26	0.42
ER1A	-	-	-	-	-	-	-	-
ER1B	-	-	-	-	-	-	-	-
ER1C	-29	14	7	-107	5.6	-0.30	-0.35	-0.49
ER2A	-31	26	35	-236	7.9	-0.33	-0.63	-1.08
ER2B	-23	23	59	-205	7.9	-0.24	-0.49	-0.94
ER3A	15	35	60	-302	9.1	0.16	-0.74	-1.38
ER3B	-41	26	42	-188	5.7	-0.43	-0.65	-0.86

Duration 1024 seconds. $\bar{u}_{10} = 12.4\ ms^{-1}$; $\bar{u}_5 = 10.8\ ms^{-1}$; $\bar{u}_3 = 9.5\ ms^{-1}$

$\bar{\beta} = 180^o$. $\sigma_{u_{10}} = 2.1\ ms^{-1}$; $\sigma_{u_5} = 2.0\ ms^{-1}$; $\sigma_{u_3} = 2.0\ ms^{-1}$

$\bar{\theta} = 208^o$. $\hat{u}_{10} = 18.9\ ms^{-1}$; $\hat{u}_5 = 17.5\ ms^{-1}$; $\hat{u}_3 = 16.2\ ms^{-1}$

Table 3 Record A35G

	$\bar{p}$ (Nm^{-2})	σ_p (Nm^{-2})	p_{max} (Nm^{-2})	p_{min} (Nm^{-2})	g (1/32 sec)	$C_{\bar{p}}$	$C_{\hat{p}}$ (2 sec)	$C_{\hat{p}}$ (1/32 sec)
3WW1	12	10	92	-35	8.0	0.16	0.28	0.43
3WW2	13	10	84	-70	8.3	0.17	0.29	0.39
3WW3	22	11	103	-49	7.4	0.29	0.32	0.47
3WW4	23	14	109	-42	6.1	0.30	0.37	0.50
3WW5	22	14	88	-62	6.0	0.28	0.33	0.41
3WW6	36	31	159	-206	7.8	0.47	0.56	-0.95
3WW7	18	32	139	-216	7.3	0.24	0.45	-1.00
5WW1	35	14	120	-9	6.1	0.45	0.41	0.55
5WW2	30	14	123	-9	6.6	0.39	0.44	0.57
5WW3	42	17	147	-11	6.2	0.54	0.51	0.68
5WW4	50	20	160	-14	5.5	0.64	0.57	0.74
5WW5	57	23	170	-50	4.9	0.74	0.61	0.79
5WW6	56	29	188	-167	7.7	0.72	0.65	0.87
5WW7	43	40	189	-156	5.0	0.55	0.70	0.87
3EW1	-37	13	-9	-103	5.1	-0.47	-0.36	-0.47
3EW2	-39	14	-10	-105	4.7	-0.50	-0.42	-0.48
3EW3	-37	14	-10	-111	5.3	-0.48	-0.41	-0.51
3EW4	-31	12	-3	-87	4.7	-0.40	-0.34	-0.40
3EW5	-29	12	1	-94	5.4	-0.38	-0.35	-0.43
5EW1	-22	9.8	4	-75	5.4	-0.28	-0.28	-0.35
5EW2	-29	11	-8	-86	5.2	-0.37	-0.35	-0.40
5EW3	-30	13	-2	-106	5.8	-0.39	-0.36	-0.49
5EW4	-24	12	5	-107	6.9	-0.31	-0.29	-0.49
5EW5	-19	13	9	-99	6.2	-0.25	-0.27	-0.46
3SW1	47	24	171	-100	6.1	0.61	0.59	0.79
3SW2	48	22	161	-83	6.0	0.62	0.64	0.74
3SW3	16	13	79	-40	4.8	0.21	0.30	0.36
3SW4	18	12	106	-26	7.3	0.23	0.33	0.49
5SW1	-35	32	107	-163	4.4	-0.45	-0.46	-0.75
5SW2	11	10	90	-11	7.9	0.14	0.30	0.42
3NW1	-19	7.4	-1	-51	4.3	-0.25	-0.20	-0.24
3NW2	-22	8.8	3	-69	5.3	-0.28	-0.24	-0.32
INT	12	7.2	42	-13	4.2	0.15	0.14	0.19
OH-U	-16	28	55	-162	5.2	-0.21	-0.51	-0.75
OH-L	40	19	141	-5	5.3	0.52	0.54	0.65
WR1A	9	15	76	-204	14.2	0.12	-0.35	-0.94
WR1B	1	18	63	-164	9.2	0.01	-0.36	-0.76
WR1C	-5	18	54	-147	8.4	-0.06	-0.47	-0.68
WR1E	-39	7.7	86	-124	16.2	-0.50	-0.32	-0.57
WR1F	-0	12	49	-165	13.7	-0.00	-0.18	-0.76
WR2C	17	13	55	-82	7.6	0.22	0.20	-0.38
WR2E	5	9.2	52	-82	9.5	0.06	0.13	-0.38
WR3A	-41	31	62	-266	7.3	-0.53	-0.72	-1.22
WR3B	17	9.7	61	-58	7.7	0.22	0.18	0.28
WR3C	25	13	71	-39	4.9	0.32	0.25	0.33
WR3D	11	16	71	-87	6.1	0.14	0.22	-0.40
WR3E	28	14	86	-26	4.1	0.36	0.27	0.40
WR4C	35	16	136	-53	6.3	0.45	0.31	0.63
ER1A	-	-	-	-	-	-	-	-
ER1B	-	-	-	-	-	-	-	-
ER1C	-23	8.8	3	-105	9.3	-0.30	-0.25	-0.48
ER2A	-26	24	13	-189	6.8	-0.34	-0.67	-0.87
ER2B	-0	19	88	-81	4.6	-0.00	0.21	0.41
ER3A	65	41	127	-251	7.7	0.84	-0.44	-1.16
ER3B	-22	23	54	-201	7.8	-0.28	-0.60	-0.93

Duration 1024 seconds. $\bar{u}_{10} = 11.2\ ms^{-1}$; $\bar{u}_5 = 9.6\ ms^{-1}$; $\bar{u}_3 = 8.4\ ms^{-1}$

$\bar{\beta} = 180^o$. $\sigma_{u10} = 2.5\ ms^{-1}$; $\sigma_{u5} = 2.4\ ms^{-1}$; $\sigma_{u3} = 2.3\ ms^{-1}$

$\bar{\theta} = 208^o$. $\hat{u}_{10} = 18.8\ ms^{-1}$; $\hat{u}_5 = 16.6\ ms^{-1}$; $\hat{u}_3 = 15.5\ ms^{-1}$

Table 4 Record A35H

	$\bar{p}$ (Nm^{-2})	σ_p (Nm^{-2})	p_{max} (Nm^{-2})	p_{min} (Nm^{-2})	g (1/32 sec)	$C_{\bar{p}}$	$C_{\hat{p}}$ (2 sec)	$C_{\hat{p}}$ (1/32 sec)
3WW1	8	8.9	65	-63	8.0	0.11	0.21	0.37
3WW2	8	8.3	61	-24	6.4	0.11	0.22	0.34
3WW3	15	9.1	59	-19	4.8	0.20	0.26	0.33
3WW4	17	11	71	-39	4.9	0.22	0.28	0.40
3WW5	16	11	80	-56	6.5	0.21	0.29	0.45
3WW6	26	30	164	-132	5.3	0.34	0.58	0.92
3WW7	3	29	128	-152	5.3	0.04	0.42	0.72
5WW1	27	12	95	-11	5.7	0.35	0.34	0.54
5WW2	32	12	102	-0	5.8	0.42	0.42	0.57
5WW3	38	14	120	3	5.9	0.50	0.44	0.68
5WW4	46	16	122	1	4.7	0.61	0.50	0.69
5WW5	51	19	127	-49	5.3	0.67	0.59	0.72
5WW6	48	26	139	-92	5.4	0.63	0.64	0.78
5WW7	32	37	152	-124	4.2	0.42	0.73	0.86
3EW1	-40	11	-9	-85	4.1	-0.53	-0.41	-0.48
3EW2	-44	12	-15	-87	3.6	-0.58	-0.43	-0.49
3EW3	-41	12	-10	-92	4.2	-0.54	-0.43	-0.52
3EW4	-35	11	-2	-80	4.1	-0.46	-0.36	-0.45
3EW5	-30	10	3	-79	4.9	-0.39	-0.34	-0.44
5EW1	-25	7.9	1	-68	5.4	-0.33	-0.28	-0.38
5EW2	-32	8.7	-9	-68	4.1	-0.32	-0.33	-0.38
5EW3	-34	11	-6	-142	9.8	-0.45	-0.37	-0.80
5EW4	-25	10	3	-119	9.4	-0.33	-0.33	-0.67
5EW5	-22	9.8	4	-97	7.7	-0.29	-0.25	-0.55
3SW1	40	22	138	-117	7.1	0.53	0.60	0.78
3SW2	45	22	145	-104	6.8	0.59	0.67	0.82
3SW3	14	13	72	-51	5.0	0.18	0.32	0.41
3SW4	17	12	73	-24	4.7	0.22	0.31	0.41
5SW1	13	30	126	-174	6.2	0.17	-0.79	-0.98
5SW2	7	8.7	63	-14	6.4	0.09	0.23	0.36
3NW1	-19	5.6	-2	-39	3.6	-0.25	-0.20	-0.22
3NW2	-21	6.7	0	-52	4.6	-0.28	-0.21	-0.29
INT	14	6.3	42	-17	4.9	0.18	0.17	0.24
OH-U	-16	24	68	-206	7.9	-0.21	-0.65	-1.16
OH-L	42	15	126	8	5.6	0.55	0.52	0.71
WR1A	-10	14	45	-111	7.2	-0.13	-0.25	-0.63
WR1B	-6	16	45	-134	8.0	-0.08	-0.45	-0.76
WR1C	-2	17	48	-126	7.3	-0.03	-0.44	-0.71
WR1E	-4	18	65	-172	9.3	-0.05	-0.53	-0.97
WR1F	1	9.6	40	-120	12.6	0.01	-0.21	-0.68
WR2C	18	14	56	-96	8.1	0.24	-0.29	-0.54
WR2E	5	11	49	-133	12.5	0.07	-0.36	-0.75
WR3A	-45	33	52	-258	6.5	-0.59	-0.83	-1.45
WR3B	47	24	144	-105	6.3	0.62	0.54	0.81
WR3C	33	13	75	-51	6.5	0.43	0.36	0.42
WR3D	21	15	78	-74	6.3	0.28	0.31	0.44
WR3E	35	14	85	-37	5.1	0.46	0.37	0.48
WR4C	43	15	114	-27	4.7	0.57	0.41	0.64
ER1A	-	-	-	-	-	-	-	-
ER1B	-	-	-	-	-	-	-	-
ER1C	19	6.1	1	-58	12.6	0.25	-0.21	-0.33
ER2A	15	16	30	-168	11.4	0.19	-0.56	-0.95
ER2B	15	20	92	-66	4.0	0.19	0.34	0.52
ER3A	4	22	42	-173	8.0	0.05	-0.43	-0.98
ER3B	20	13	63	-84	8.0	0.26	-0.34	-0.47

Duration 1024 seconds. $\bar{u}_{10} = 11.1\ ms^{-1}$; $\bar{u}_5 = 9.6\ ms^{-1}$; $\bar{u}_3 = 8.3\ ms^{-1}$

$\bar{\beta} = 180^o$. $\sigma_{u_{10}} = 2.2\ ms^{-1}$; $\sigma_{u_5} = 2.2\ ms^{-1}$; $\sigma_{u_3} = 2.1\ ms^{-1}$

$\bar{\theta} = 208^o$. $\hat{u}_{10} = 17.0\ ms^{-1}$; $\hat{u}_5 = 15.7\ ms^{-1}$; $\hat{u}_3 = 14.3\ ms^{-1}$

Table 5 Record A35J

	$\bar{p}$ (Nm^{-2})	σ_p (Nm^{-2})	p_{max} (Nm^{-2})	p_{min} (Nm^{-2})	g (1/32 sec)	$C_{\bar{p}}$	$C_{\hat{p}}$ (2 sec)	$C_{\hat{p}}$ (1/32 sec)
3WW1	9	11	64	-22	5.0	0.13	0.35	0.53
3WW2	11	11	73	-18	5.6	0.16	0.39	0.61
3WW3	18	12	99	-18	6.7	0.27	0.57	0.82
3WW4	21	15	106	-25	5.7	0.31	0.70	0.88
3WW5	20	13	109	-44	6.8	0.30	0.60	0.91
3WW6	39	26	207	-120	6.5	0.58	1.02	1.72
3WW7	19	29	158	-114	4.8	0.28	0.85	1.32
5WW1	35	14	110	-51	6.1	0.52	0.68	0.92
5WW2	33	15	127	-3	6.3	0.49	0.74	1.06
5WW3	43	18	140	-0	5.4	0.64	0.88	1.16
5WW4	51	20	143	-7	4.6	0.76	0.97	1.19
5WW5	58	23	153	-33	4.1	0.86	1.12	1.28
5WW6	55	26	166	-47	4.3	0.82	1.14	1.39
5WW7	47	37	171	-116	4.4	0.70	1.21	1.43
3EW1	-43	11	-13	-84	3.7	-0.64	-0.58	-0.70
3EW2	-46	12	-16	-88	3.5	-0.69	-0.65	-0.73
3EW3	-43	11	-12	-90	4.3	-0.64	-0.58	-0.75
3EW4	-35	9.8	-5	-80	4.6	-0.52	-0.52	-0.67
3EW5	-30	9.1	2	-70	4.4	-0.45	-0.43	-0.58
5EW1	-26	7.7	-6	-63	4.8	-0.39	-0.38	-0.53
5EW2	-33	8.4	-13	-68	4.2	-0.49	-0.47	-0.57
5EW3	-35	10	-8	-89	5.4	-0.52	-0.52	-0.74
5EW4	-26	9.0	-5	-76	5.6	-0.39	-0.38	-0.63
5EW5	-20	8.2	5	-67	5.7	-0.30	-0.33	-0.56
3SW1	36	21	142	-111	7.0	0.53	0.87	1.18
3SW2	40	19	156	-61	6.1	0.60	0.95	1.30
3SW3	3	11	53	-48	4.6	0.04	0.30	0.44
3SW4	8	11	72	-29	5.8	0.12	0.38	0.60
5SW1	4	28	109	-112	4.1	0.06	0.68	0.91
5SW2	7	7	61	-10	7.7	0.10	0.33	0.51
3NW1	-19	5.8	-3	-43	4.1	-0.28	-0.28	-0.36
3NW2	-22	7.0	0	-51	4.1	-0.33	-0.34	-0.43
INT	11	6.3	33	-17	4.4	0.16	0.21	0.28
OH-U	-55	26	20	-194	5.3	-0.82	-1.30	-1.62
OH-L	46	19	148	-13	5.4	0.69	0.92	1.23
WR1A	10	22	65	-180	8.6	0.15	-0.77	-1.50
WR1B	-16	25	45	-178	6.5	-0.24	-1.10	-1.49
WR1C	-22	21	46	-174	7.2	-0.33	-0.93	-1.45
WR1E	-8	25	66	-204	7.8	-0.12	-0.82	-1.70
WR1F	1	11	50	-109	10.0	0.01	-0.32	-0.91
WR2C	13	19	56	-121	7.1	0.19	-0.66	-1.01
WR2E	-2	14	44	-104	7.3	-0.03	-0.49	-0.87
WR3A	-63	31	40	-227	5.3	-0.94	-1.34	-1.90
WR3B	42	19	112	-102	7.6	0.63	0.72	0.93
WR3C	31	13	74	-54	6.5	0.46	0.53	0.62
WR3D	14	16	66	-90	6.5	0.21	0.41	-0.75
WR3E	34	14	90	-37	5.1	0.51	0.57	0.75
WR4C	45	14	90	-50	6.8	0.67	0.65	0.75
ER1A	-	-	-	-	-	-	-	-
ER1B	-	-	-	-	-	-	-	-
ER1C	-21	6.1	-0	-54	5.4	-0.31	-0.30	-0.45
ER2A	-12	18	31	-188	9.8	-0.18	-0.93	-1.57
ER2B	24	21	95	-66	4.3	0.36	0.58	0.79
ER3A	68	7.5	83	17	6.8	1.01	0.64	0.69
ER3B	34	13	83	-25	4.5	0.50	0.56	0.69

Duration 1024 seconds. $\bar{u}_{10} = 10.4\ ms^{-1}$; $\bar{u}_5 = 9.1\ ms^{-1}$; $\bar{u}_3 = 7.9\ ms^{-1}$

$\bar{\beta} = 180^o$. $\sigma_{u10} = 1.9\ ms^{-1}$; $\sigma_{u5} = 1.9\ ms^{-1}$; $\sigma_{u3} = 1.9\ ms^{-1}$

$\bar{\theta} = 208^o$. $\hat{u}_{10} = 14.0\ ms^{-1}$; $\hat{u}_5 = 13.3\ ms^{-1}$; $\hat{u}_3 = 12.4\ ms^{-1}$

Table 6 Record A38A

	$\bar{p}$ (Nm^{-2})	σ_p (Nm^{-2})	p_{max} (Nm^{-2})	p_{min} (Nm^{-2})	g (1/32 sec)	$C_{\bar{p}}$	$C_{\hat{p}}$ (2 sec)	$C_{\hat{p}}$ (1/32 sec)
3WW1	6	27	370	-73	13.5	0.06	0.76	1.35
3WW2	15	24	299	-50	11.8	0.16	0.60	1.09
3WW3	23	25	269	-36	9.8	0.24	0.57	0.99
3WW4	26	27	307	-44	10.4	0.28	0.63	1.13
3WW5	23	27	294	-66	10.0	0.24	0.54	1.08
3WW6	46	39	358	-307	8.0	0.49	0.65	1.31
3WW7	32	31	250	-236	8.6	0.34	0.59	0.92
5WW1	47	32	389	-28	10.7	0.50	0.96	1.43
5WW2	51	34	357	-23	9.0	0.54	1.07	1.31
5WW3	59	35	369	-5	8.9	0.63	1.02	1.35
5WW4	65	36	359	-23	8.2	0.69	0.98	1.32
5WW5	71	38	266	-16	5.1	0.76	0.83	0.98
5WW6	69	38	355	-97	7.5	0.73	0.84	1.30
5WW7	63	38	307	-158	6.4	0.67	0.80	1.13
3EW1	-50	18	-7	-139	4.9	-0.53	-0.46	-0.51
3EW2	-54	20	-8	-180	6.3	-0.57	-0.57	-0.66
3EW3	-49	17	-6	-180	7.7	-0.52	-0.51	-0.66
3EW4	-44	15	-3	-136	6.1	-0.47	-0.39	-0.50
3EW5	-44	16	-2	-124	5.0	-0.47	-0.36	-0.45
5EW1	-36	14	0	-104	4.9	-0.38	-0.33	-0.38
5EW2	-40	15	-4	-152	7.5	-0.43	-0.44	-0.56
5EW3	-48	18	-4	-187	7.7	-0.51	-0.49	-0.69
5EW4	-39	14	2	-127	6.3	-0.42	-0.30	-0.47
5EW5	-38	16	8	-135	6.1	-0.40	-0.29	-0.50
3SW1	-15	47	408	-238	4.7	-0.16	-0.52	-0.87
3SW2	-44	44	348	-336	7.3	-0.47	-0.73	-1.34
3SW3	-23	18	83	-205	10.1	-0.24	-0.44	-0.75
3SW4	-16	14	107	-116	8.8	-0.17	-0.21	-0.43
5SW1	-1	55	265	-223	4.8	-0.01	0.52	0.97
5SW2	12	44	188	-173	4.2	0.13	0.45	0.69
3NW1	-36	14	4	-236	14.3	-0.38	-0.55	-0.87
3NW2	-43	19	5	-310	14.0	-0.46	-0.87	-1.14
INT	-7	10	58	-119	11.2	-0.07	-0.20	-0.44
OH-U	-59	39	83	-305	6.3	-0.63	-0.61	-1.12
OH-L	56	35	417	-23	10.3	0.60	0.95	1.53
WR1A	-42	70	97	-567	7.5	-0.45	-1.06	-2.08
WR1B	-92	78	102	-591	6.4	-0.98	-1.24	-2.17
WR1C	-79	48	77	-441	7.5	-0.84	-0.77	-1.62
WR1E	10	35	177	-298	8.8	0.11	-0.41	-1.09
WR1F	-27	25	55	-342	12.6	-0.29	-0.52	-1.25
WR2C	-18	41	88	-253	5.7	-0.19	-0.61	-0.93
WR2E	-2	18	131	-129	7.1	-0.02	-0.30	-0.47
WR3A	-5	26	87	-325	12.3	-0.05	-0.52	-1.19
WR3B	11	19	154	-178	9.9	0.12	-0.08	-0.65
WR3C	4	18	125	-148	8.4	0.04	-0.22	-0.54
WR3D	-4	22	113	-160	7.1	-0.04	-0.22	-0.59
WR3E	5	16	84	-66	4.9	0.05	0.19	0.31
WR4C	11	18	119	-54	6.0	0.12	0.23	0.44
ER1A	-58	24	13	-219	6.7	-0.62	-0.49	-0.80
ER1B	-49	16	-5	-178	8.1	-0.52	-0.37	-0.65
ER1C	-45	17	9	-225	10.6	-0.48	-0.37	-0.83
ER2A	-61	39	38	-375	8.1	-0.65	-0.83	-1.38
ER2B	-16	23	84	-140	5.4	-0.17	-0.26	-0.51
ER3A	10	62	121	-355	5.9	0.11	-0.59	-1.30
ER3B	-44	41	56	-299	6.2	-0.47	-0.66	-1.10

Duration 1024 seconds. $\bar{u}_{10} = 12.4\ ms^{-1}$; $\bar{u}_5 = 10.5\ ms^{-1}$; $\bar{u}_3 = 9.5\ ms^{-1}$

$\bar{\beta} = 205^o$. $\sigma_{u_{10}} = 2.8\ ms^{-1}$; $\sigma_{u_5} = 2.6\ ms^{-1}$; $\sigma_{u_3} = 2.5\ ms^{-1}$

$\bar{\theta} = 233^o$. $\hat{u}_{10} = 21.1\ ms^{-1}$; $\hat{u}_5 = 21.0\ ms^{-1}$; $\hat{u}_3 = 21.0\ ms^{-1}$

Table 7 Record A38B

	$\bar{p}$ (Nm^{-2})	σ_p (Nm^{-2})	p_{max} (Nm^{-2})	p_{min} (Nm^{-2})	g (1/32 sec)	$C_{\bar{p}}$	$C_{\hat{p}}$ (2 sec)	$C_{\hat{p}}$ (1/32 sec)
3WW1	8	20	188	-87	9.0	0.10	0.37	0.73
3WW2	13	18	126	-48	6.3	0.17	0.32	0.49
3WW3	19	19	143	-34	6.5	0.24	0.40	0.56
3WW4	23	21	171	-41	7.0	0.29	0.49	0.67
3WW5	28	21	158	-25	6.2	0.36	0.48	0.62
3WW6	41	31	229	-144	6.1	0.52	0.61	0.89
3WW7	31	27	165	-171	5.0	0.39	0.43	0.64
5WW1	34	22	196	-42	7.4	0.43	0.44	0.76
5WW2	43	25	206	-48	6.5	0.55	0.52	0.80
5WW3	49	26	212	-10	6.3	0.62	0.59	0.83
5WW4	56	28	223	-1	6.0	0.71	0.68	0.87
5WW5	63	31	234	-10	5.5	0.80	0.73	0.91
5WW6	61	32	236	-106	5.5	0.78	0.68	0.92
5WW7	58	34	213	-139	4.6	0.74	0.61	0.83
3EW1	-40	17	-5	-116	4.5	-0.51	-0.40	-0.45
3EW2	-44	19	-8	-127	4.4	-0.56	-0.44	-0.50
3EW3	-41	17	-9	-119	4.6	-0.52	-0.39	-0.46
3EW4	-35	14	-3	-98	4.5	-0.45	-0.30	-0.38
3EW5	-34	14	11	-99	4.6	-0.43	-0.31	-0.39
5EW1	-28	13	3	-94	5.1	-0.36	-0.28	-0.37
5EW2	-34	14	-2	-99	4.6	-0.43	-0.33	-0.39
5EW3	-35	15	-0	-144	7.3	-0.45	-0.32	-0.56
5EW4	-31	14	0	-142	7.9	-0.39	-0.30	-0.55
5EW5	-29	14	10	-119	6.4	-0.37	-0.29	-0.46
3SW1	1	40	324	-185	8.1	0.01	0.48	-0.72
3SW2	6	36	172	-207	5.9	0.08	0.43	-0.81
3SW3	-14	13	65	-94	6.1	-0.18	0.13	-0.37
3SW4	-9	12	81	-75	7.5	-0.11	0.13	-0.29
5SW1	5	50	361	-207	7.1	0.06	0.60	-0.81
5SW2	24	39	209	-143	4.7	0.31	0.52	-0.56
3NW1	-27	11	7	-91	5.8	-0.34	-0.28	-0.36
3NW2	-34	14	4	-164	9.3	-0.43	-0.39	-0.64
INT	0	10	53	-38	5.3	0	0.11	0.21
OH-U	-64	36	39	-261	5.5	-0.81	-0.75	-1.02
OH-L	47	26	229	-10	7.0	0.60	0.57	0.89
WR1A	-59	74	51	-641	7.9	-0.75	-1.81	-2.50
WR1B	-108	78	65	-580	6.1	-1.37	-1.41	-2.26
WR1C	-90	42	50	-401	7.4	-1.14	-1.01	-1.56
WR1E	1	30	96	-234	7.8	0.01	-0.42	-0.91
WR1F	-19	23	55	-218	8.7	-0.24	-0.33	-0.85
WR2C	-18	44	91	-278	5.9	-0.23	-0.75	-1.08
WR2E	-7	16	57	-124	7.3	-0.09	-0.24	-0.48
WR3A	-10	28	102	-427	14.9	-0.13	-0.62	-1.67
WR3B	14	22	148	-132	6.6	0.18	-0.15	-0.58
WR3C	6	23	90	-139	6.3	0.08	-0.23	-0.54
WR3D	-3	28	91	-156	5.5	-0.04	-0.38	-0.61
WR3E	12	20	95	-62	4.1	0.15	0.25	0.37
WR4C	17	20	89	-44	3.6	0.22	0.25	0.35
ER1A	-40	20	-0	-162	6.1	-0.51	-0.40	-0.63
ER1B	-35	13	2	-118	6.4	-0.46	-0.30	-0.46
ER1C	-33	13	3	-179	11.2	-0.42	-0.24	-0.70
ER2A	-48	36	19	-339	8.1	-0.61	-0.84	-1.32
ER2B	4	21	82	-72	3.7	0.05	-0.13	-0.28
ER3A	7	38	62	-340	9.1	0.09	-0.52	-1.33
ER3B	-11	33	79	-167	4.7	-0.14	-0.43	-0.65

Duration 1024 seconds. $\bar{u}_{10} = 11.3\ ms^{-1}$; $\bar{u}_5 = 9.5\ ms^{-1}$; $\bar{u}_3 = 8.3\ ms^{-1}$

$\bar{\beta} = 205^{o}$. $\sigma_{u_{10}} = 3.1\ ms^{-1}$; $\sigma_{u_5} = 2.8\ ms^{-1}$; $\sigma_{u_3} = 2.7\ ms^{-1}$

$\bar{\theta} = 233^{o}$. $\hat{u}_{10} = 20.4\ ms^{-1}$; $\hat{u}_5 = 19.3\ ms^{-1}$; $\hat{u}_3 = 16.1\ ms^{-1}$

Table 8 Record A38C

	$\bar{p}$ (Nm^{-2})	σ_p (Nm^{-2})	p_{max} (Nm^{-2})	p_{min} (Nm^{-2})	g (1/32 sec)	$C_{\bar{p}}$	$C_{\hat{p}}$ (2 sec)	$C_{\hat{p}}$ (1/32 sec)
3WW1	11	21	148	-79	6.5	0.15	0.35	0.71
3WW2	17	19	130	-43	5.9	0.22	0.39	0.63
3WW3	22	20	124	-46	5.1	0.29	0.41	0.60
3WW4	28	23	158	-32	5.7	0.37	0.48	0.76
3WW5	30	22	161	-35	6.0	0.40	0.50	0.78
3WW6	40	33	249	-48	6.3	0.53	0.75	1.20
3WW7	30	26	209	-48	6.9	0.40	0.63	1.01
5WW1	37	25	226	-37	7.6	0.49	0.55	1.09
5WW2	45	26	215	-5	6.5	0.60	0.67	1.04
5WW3	52	27	206	-2	5.7	0.69	0.69	0.99
5WW4	56	29	226	-23	5.9	0.74	0.68	1.09
5WW5	61	32	248	-4	5.8	0.81	0.78	1.19
5WW6	59	32	280	-10	6.9	0.78	0.87	1.35
5WW7	57	33	307	-51	7.6	0.75	0.93	1.48
3EW1	-37	15	-5	-125	5.9	-0.49	-0.50	-0.60
3EW2	-42	17	-7	-129	5.1	-0.56	-0.54	0.62
3EW3	-39	16	-5	-131	5.7	-0.52	-0.52	0.63
3EW4	-33	13	1	-113	6.2	-0.44	-0.48	0.54
3EW5	-31	13	5	-105	5.7	-0.41	-0.41	0.51
5EW1	-27	12	4	-98	5.9	-0.36	-0.35	-0.47
5EW2	-34	13	-6	-106	5.5	-0.45	-0.41	-0.51
5EW3	-34	14	-1	-113	5.6	-0.45	-0.43	-0.54
5EW4	-31	14	0	-111	5.7	-0.41	-0.40	-0.53
5EW5	-29	14	8	-135	7.6	-0.38	-0.38	-0.65
3SW1	-7	39	192	-252	6.3	-0.09	-0.47	-1.21
3SW2	-0	36	178	-230	6.4	-0.00	-0.53	-1.11
3SW3	-16	13	76	-98	6.3	-0.21	-0.37	-0.47
3SW4	-8	12	73	-68	5.0	-0.11	-0.19	-0.33
5SW1	-3	46	358	-260	7.8	-0.04	0.79	1.72
5SW2	17	37	212	-166	5.3	0.22	0.69	1.02
3NW1	-26	11	2	-87	5.5	-0.34	-0.36	-0.42
3NW2	-33	15	10	-205	11.5	-0.44	-0.48	-0.99
INT	1	10	42	-44	4.5	0.01	0.14	0.20
OH-U	-74	40	26	-316	6.0	-0.98	-1.00	-1.52
OH-L	45	28	211	-16	5.9	0.60	0.66	1.02
WR1A	-94	91	39	-622	5.8	-1.24	-1.95	-2.99
WR1B	-117	75	38	-679	7.5	-1.54	-1.92	-3.27
WR1C	-91	41	12	-493	9.8	-1.20	-1.29	-2.37
WR1E	-17	38	90	-357	8.9	-0.22	-0.63	-1.72
WR1F	-24	30	47	-225	6.7	-0.32	-0.63	-1.08
WR2C	-35	46	85	-253	4.7	-0.46	-0.85	-1.22
WR2E	-14	22	48	-211	8.9	-0.18	-0.44	-1.02
WR3A	-15	24	66	-278	11.0	-0.20	-0.66	-1.34
WR3B	9	23	116	-256	11.5	0.12	-0.37	-1.23
WR3C	-2	29	103	-231	7.9	-0.03	-0.52	-1.11
WR3D	-14	30	107	-223	7.0	-0.19	-0.51	-1.07
WR3E	10	20	97	-84	4.7	0.13	0.35	0.47
WR4C	26	19	96	-80	5.6	0.34	0.42	0.46
ER1A	-30	17	14	-185	9.1	-0.40	-0.49	-0.89
ER1B	-26	14	9	-101	5.4	-0.34	-0.36	-0.49
ER1C	-31	13	3	-119	6.8	-0.41	-0.36	-0.57
ER2A	-35	29	34	-353	11.0	-0.46	-1.08	-1.70
ER2B	8	20	109	-63	5.0	0.11	0.34	0.52
ER3A	31	23	83	-199	10.0	0.41	-0.32	-0.96
ER3B	17	21	101	-52	4.0	0.22	0.40	0.49

Duration 1024 seconds. $\bar{u}_{10} = 11.1\ ms^{-1}$; $\bar{u}_5 = 9.4\ ms^{-1}$; $\bar{u}_3$ 8.2 ms^{-1}

$\bar{\beta} = 205^o$. $\sigma_{u_{10}} = 2.7\ ms^{-1}$; $\sigma_{u_5} = 2.6\ ms^{-1}$; $\sigma_{u_3} = 2.5\ ms^{-1}$

$\bar{\theta} = 233^o$. $\hat{u}_{10} = 18.4\ ms^{-1}$; $\hat{u}_5 = 17.1\ ms^{-1}$; $\hat{u}_3 = 17.6\ ms^{-1}$

Table 9 Record A38D

	$\bar{p}$ (Nm^{-2})	σ_p (Nm^{-2})	p_{max} (Nm^{-2})	p_{min} (Nm^{-2})	g (1/32 sec)	$C_{\bar{p}}$	$C_{\hat{p}}$ (2 sec)	$C_{\hat{p}}$ (1/32 sec)
3WW1	5	18	117	-65	6.2	0.06	0.31	0.48
3WW2	14	17	117	-47	6.1	0.17	0.35	0.48
3WW3	21	18	133	-34	6.2	0.26	0.38	0.55
3WW4	27	20	152	-50	6.2	0.33	0.40	0.63
3WW5	32	20	140	-85	5.4	0.40	0.36	0.58
3WW6	45	30	178	-165	7.0	0.56	0.56	0.74
3WW7	35	27	158	-177	7.8	0.43	0.48	0.65
5WW1	5	11	130	-15	11.4	0.06	0.32	0.54
5WW2	50	24	221	-11	7.1	0.62	0.65	0.91
5WW3	47	24	194	-33	6.1	0.58	0.65	0.80
5WW4	53	25	198	-19	5.8	0.65	0.68	0.82
5WW5	56	26	209	-18	5.9	0.69	0.70	0.86
5WW6	54	27	188	-127	6.7	0.67	0.61	0.78
5WW7	57	30	195	-147	5.3	0.70	0.58	0.81
3EW1	-46	17	-5	-131	5.0	-0.57	-0.48	-0.54
3EW2	-48	18	-5	-144	5.3	-0.59	-0.53	-0.60
3EW3	-50	18	-8	-165	6.4	-0.62	-0.58	-0.68
3EW4	-44	17	-3	-159	6.8	-0.54	-0.55	-0.66
3EW5	-42	16	-3	-172	8.1	-0.52	-0.58	-0.71
5EW1	-38	15	-4	-109	4.7	-0.47	-0.35	-0.45
5EW2	-42	15	-8	-115	4.9	-0.52	-0.41	-0.48
5EW3	-48	18	-5	-217	9.4	-0.59	-0.60	-0.90
5EW4	-45	17	-3	-172	7.5	-0.56	-0.43	-0.71
5EW5	-45	16	-2	-137	5.7	-0.56	-0.48	-0.57
3SW1	-1	40	162	-194	4.8	-0.01	-0.43	-0.80
3SW2	5	35	165	-219	6.4	0.06	-0.45	-0.91
3SW3	5	19	130	-85	6.6	0.06	0.32	0.54
3SW4	-16	13	88	-101	8.0	-0.20	-0.36	-0.42
5SW1	44	47	301	-206	5.5	0.54	0.76	1.24
5SW2	30	41	269	-158	5.8	0.37	0.65	1.11
3NW1	-35	13	-4	-116	6.2	-0.43	-0.38	-0.48
3NW2	-41	16	4	-175	8.4	-0.51	-0.45	-0.72
INT	-12	9	34	-51	5.1	-0.15	-0.15	-0.21
OH-U	5	25	106	-113	4.4	0.06	-0.19	-0.47
OH-L	43	24	194	18	6.3	0.53	0.62	0.80
WR1A	8	32	133	-230	7.4	0.10	-0.36	-0.95
WR1B	-18	42	123	-410	9.3	-0.22	-0.65	-1.70
WR1C	-19	29	112	-229	7.2	-0.23	-0.38	-0.95
WR1E	11	22	112	-87	4.6	0.14	0.38	0.46
WR1F	-8	19	99	-126	6.2	-0.10	-0.18	-0.52
WR2C	20	19	103	-79	5.2	0.25	0.31	0.43
WR2E	22	16	114	-37	5.7	0.27	0.33	0.47
WR3A	8	17	85	-202	12.3	0.10	-0.24	-0.84
WR3B	13	12	107	-150	13.6	0.16	-0.09	-0.62
WR3C	7	9	67	-27	6.7	0.09	0.16	0.28
WR3D	6	11	71	-69	6.8	0.07	0.19	0.29
WR3E	5	11	72	-31	6.1	0.06	0.17	0.30
WR4C	-3	9.7	98	-75	10.4	-0.04	-0.17	-0.31
ER1A	-66	27	-10	-293	8.4	-0.81	-0.71	-1.21
ER1B	-58	21	2	-237	8.5	-0.72	-0.65	-0.98
ER1C	-55	19	-10	-204	7.8	-0.68	-0.48	-0.84
ER2A	-55	29	-4	-276	7.6	-0.68	-0.73	-1.14
ER2B	-52	28	52	-294	8.6	-0.64	-0.79	-1.22
ER3A	-14	41	44	-347	8.1	-0.17	-0.98	-1.44
ER3B	-41	23	29	-260	9.5	-0.51	-0.58	-1.08

Duration 1024 seconds. $\bar{u}_{10} = 11.5\ ms^{-1}$; $\bar{u}_5 = 9.7\ ms^{-1}$; $\bar{u}_3 = 8.5\ ms^{-1}$

$\bar{\beta} = 205^o$. $\sigma_{u_{10}} = 2.6\ ms^{-1}$; $\sigma_{u_5} = 2.3\ ms^{-1}$; $\sigma_{u_3} = 2.2\ ms^{-1}$

$\bar{\theta} = 233^o$. $\hat{u}_{10} = 19.9\ ms^{-1}$; $\hat{u}_5 = 17.7\ ms^{-1}$; $\hat{u}_3 = 16.1\ ms^{-1}$

Table 10 Record A38E

	$\bar{p}$ (Nm^{-2})	σ_p (Nm^{-2})	p_{max} (Nm^{-2})	p_{min} (Nm^{-2})	g (1/32 sec)	$C_{\bar{p}}$	$C_{\hat{p}}$ (2 sec)	$C_{\hat{p}}$ (1/32 sec)
3WW1	1	18	126	-66	6.9	0.01	0.23	0.61
3WW2	11	18	106	-40	5.3	0.14	0.32	0.51
3WW3	20	20	163	-29	7.1	0.25	0.42	0.79
3WW4	24	23	135	-31	4.8	0.30	0.52	0.66
3WW5	30	23	159	-24	5.6	0.38	0.57	0.77
3WW6	42	32	233	-153	6.0	0.53	0.87	1.13
3WW7	33	26	187	-126	5.9	0.42	0.71	0.91
5WW1	28	20	161	-37	6.6	0.35	0.48	0.78
5WW2	28	24	152	-26	5.2	0.35	0.51	0.74
5WW3	40	25	164	-10	5.0	0.50	0.62	0.80
5WW4	45	26	179	-24	5.1	0.57	0.69	0.87
5WW5	51	28	196	-6	5.2	0.64	0.76	0.95
5WW6	52	28	203	-57	5.4	0.65	0.74	0.99
5WW7	53	28	214	-104	5.7	0.67	0.78	1.04
3EW1	-44	16	-9	-133	5.6	-0.55	-0.54	-0.65
3EW2	-48	16	-14	-135	5.4	-0.60	-0.56	-0.66
3EW3	-51	17	-16	-136	5.0	-0.64	-0.58	-0.66
3EW4	-45	15	-9	-125	5.3	-0.57	-0.50	-0.61
3EW5	-44	16	1	-143	6.2	-0.55	-0.53	-0.69
5EW1	-39	14	-3	-125	6.1	-0.49	-0.48	-0.61
5EW2	-44	14	-9	-123	5.6	-0.55	-0.50	-0.60
5EW3	-51	17	-11	-145	5.5	-0.64	-0.59	-0.70
5EW4	-49	16	-9	-134	5.3	-0.62	-0.54	-0.65
5EW5	-48	17	4	-136	5.2	-0.60	-0.53	-0.66
3SW1	-5	38	140	-200	5.1	-0.06	-0.49	-0.97
3SW2	3	37	130	-151	4.0	0.04	-0.50	-0.73
3SW3	3	16	125	-78	7.6	0.04	-0.19	-0.38
3SW4	-14	12	60	-82	6.2	-0.18	-0.24	-0.40
5SW1	6	45	170	-197	4.2	0.08	-0.71	-0.96
5SW2	23	38	175	-167	5.0	0.29	-0.46	-0.81
3NW1	-36	13	-2	-122	6.6	-0.45	-0.41	-0.59
3NW2	-43	15	-4	-141	6.5	-0.54	-0.52	-0.68
INT	-16	9	24	-61	5.0	-0.20	-0.21	-0.30
OH-U	17	23	120	-115	5.7	0.21	0.42	0.58
OH-L	34	24	159	-18	5.2	0.43	0.57	0.77
WR1A	31	27	202	-218	9.2	0.39	-0.23	-1.06
WR1B	18	31	187	-133	5.4	0.23	0.48	0.91
WR1C	11	25	150	-143	6.2	0.14	0.42	0.73
WR1E	-35	26	87	-113	4.7	-0.44	-0.38	-0.55
WR1F	-4	19	85	-113	5.7	-0.05	-0.18	-0.55
WR2C	32	17	137	-74	6.2	0.40	0.41	0.67
WR2E	29	20	140	-24	5.6	0.37	0.47	0.68
WR3A	16	15	99	-227	16.2	0.20	0.28	-1.10
WR3B	15	11	93	-70	7.7	0.19	0.23	0.45
WR3C	10	8.8	65	-20	6.2	0.13	0.17	0.31
WR3D	8	10	67	-31	5.9	0.10	0.17	0.33
WR3E	7	11	142	-32	12.2	0.09	0.16	0.69
WR4C	-21	7.5	85	-63	14.1	-0.26	-0.18	-0.31
ER1A	-52	20	-8	-207	7.7	-0.65	-0.73	-1.00
ER1B	-59	19	-18	-166	5.6	-0.74	-0.61	-0.81
ER1C	-62	20	-20	-175	5.6	-0.78	-0.59	-0.85
ER2A	-43	18	6	-199	8.7	-0.54	-0.65	-0.97
ER2B	-47	20	3	-188	7.0	-0.59	-0.68	-0.91
ER3A	-14	17	26	-142	7.5	-0.18	-0.52	-0.69
ER3B	-41	20	16	-171	6.5	-0.52	-0.59	-0.83

Duration 1024 seconds. $\bar{u}_{10} = 11.4\ ms^{-1}$; $\bar{u}_5 = 9.6\ ms^{-1}$; $\bar{u}_3 = 8.3\ ms^{-1}$

$\bar{\beta} = 205^o$. $\sigma_{u_{10}} = 2.6\ ms^{-1}$; $\sigma_{u_5} = 2.4\ ms^{-1}$; $\sigma_{u_3} = 2.3\ ms^{-1}$

$\bar{\theta} = 233^o$. $\hat{u}_{10} = 18.3\ ms^{-1}$; $\hat{u}_5 = 16.7\ ms^{-1}$; $\hat{u}_3 = 14.9\ ms^{-1}$

Table 11 Record A38F

	$\bar{p}$ (Nm^{-2})	σ_p (Nm^{-2})	p_{max} (Nm^{-2})	p_{min} (Nm^{-2})	g (1/32 sec)	$C_{\bar{p}}$	$C_{\hat{p}}$ (2 sec)	$C_{\hat{p}}$ (1/32 sec)
3WW1	6	19	107	-80	5.3	0.09	0.32	0.49
3WW2	17	17	99	-56	4.8	0.27	0.34	0.45
3WW3	21	19	101	-30	4.2	0.33	0.36	0.46
3WW4	27	21	124	-23	4.6	0.43	0.43	0.57
3WW5	30	20	123	-25	4.6	0.47	0.45	0.57
3WW6	33	27	172	-42	5.1	0.52	0.58	0.79
3WW7	18	20	139	-40	6.0	0.28	0.42	0.64
5WW1	31	20	152	-59	6.0	0.49	0.48	0.70
5WW2	47	25	176	-85	5.2	0.74	0.64	0.81
5WW3	50	25	178	-35	5.1	0.79	0.58	0.82
5WW4	49	26	170	-23	4.6	0.77	0.58	0.78
5WW5	46	27	175	-9	4.8	0.73	0.62	0.80
5WW6	48	26	181	-4	5.1	0.76	0.62	0.83
5WW7	39	23	166	-16	5.5	0.62	0.54	0.76
3EW1	-35	14	-6	-109	5.3	-0.55	-0.44	-0.50
3EW2	-38	14	-8	-110	5.1	-0.60	-0.43	-0.51
3EW3	-39	15	-6	-132	6.2	-0.62	-0.50	-0.61
3EW4	-37	13	-8	-117	6.1	-0.59	-0.44	-0.54
3EW5	-42	16	0	-119	4.8	-0.66	-0.45	-0.55
5EW1	-28	12	-1	-88	5.0	-0.44	-0.36	-0.40
5EW2	-34	12	-8	-94	5.0	-0.54	-0.40	-0.43
5EW3	-38	15	-5	-120	5.5	-0.60	-0.49	-0.55
5EW4	-39	14	-5	-114	5.4	-0.62	-0.44	-0.52
5EW5	-46	16	-5	-125	4.9	-0.73	-0.49	-0.57
3SW1	-47	28	65	-244	7.0	-0.74	-0.48	-1.12
3SW2	-42	30	53	-198	5.2	-0.66	-0.52	-0.91
3SW3	-23	17	33	-134	6.5	-0.36	-0.35	-0.62
3SW4	-24	11	10	-84	5.5	-0.38	-0.26	-0.39
5SW1	1	32	158	-165	5.2	0.01	-0.38	-0.76
5SW2	-37	34	118	-177	4.6	-0.59	-0.54	-0.81
3NW1	-47	17	-3	-135	5.2	-0.74	-0.49	-0.62
3NW2	-57	20	-2	-169	5.6	-0.90	-0.61	-0.78
INT	-27	11	-3	-92	5.9	-0.43	-0.31	-0.42
OH-U	98	26	307	13	8.0	1.55	0.82	1.41
OH-L	43	23	148	-28	4.6	0.68	0.52	0.68
WR1A	38	26	207	-48	6.5	0.60	0.59	0.95
WR1B	30	33	204	-88	5.3	0.47	0.65	0.93
WR1C	41	27	184	-43	5.3	0.65	0.58	0.85
WR1E	33	33	172	-44	4.2	0.52	0.59	0.79
WR1F	12	24	129	-85	4.9	0.19	0.40	0.59
WR2C	43	24	170	-9	5.3	0.68	0.57	0.78
WR2E	52	28	182	-7	4.6	0.82	0.63	0.84
WR3A	18	15	125	-75	7.1	0.28	0.32	0.57
WR3B	20	16	120	-48	6.2	0.32	0.36	0.55
WR3C	19	15	109	-39	6.0	0.30	0.32	0.50
WR3D	19	17	121	-23	6.0	0.30	0.33	0.56
WR3E	16	17	114	-40	5.8	0.25	0.29	0.52
WR4C	-12	10	51	-90	7.8	-0.19	-0.13	-0.41
ER1A	-40	16	5	-128	5.5	-0.63	-0.46	-0.59
ER1B	-46	17	-12	-132	5.1	-0.73	-0.49	-0.61
ER1C	-50	19	-4	-183	7.0	-0.79	-0.59	-0.84
ER2A	-35	16	0	-124	5.6	-0.55	-0.41	-0.57
ER2B	-39	17	-0	-118	4.6	-0.62	-0.45	-0.54
ER3A	-16	17	13	-141	7.3	-0.25	-0.42	-0.65
ER3B	-36	16	3	-111	4.7	-0.57	-0.41	-0.51

Duration 1024 seconds. $\bar{u}_{10} = 10.2\ ms^{-1}$; $\bar{u}_5 = 8.3\ ms^{-1}$; $\bar{u}_3 = 7.1\ ms^{-1}$

$\bar{\beta} = 210^o$. $\sigma_{u_{10}} = 2.8\ ms^{-1}$; $\sigma_{u_5} = 2.4\ ms^{-1}$; $\sigma_{u_3} = 2.2\ ms^{-1}$

$\bar{\theta} = 238^o$. $\hat{u}_{10} = 18.8\ ms^{-1}$; $\hat{u}_5 = 15.9\ ms^{-1}$; $\hat{u}_3 = 14.5\ ms^{-1}$

Table 12 Record A38G

	$\bar{p}$ (Nm^{-2})	σ_p (Nm^{-2})	p_{max} (Nm^{-2})	p_{min} (Nm^{-2})	g (1/32 sec)	$C_{\bar{p}}$	$C_{\hat{p}}$ (2 sec)	$C_{\hat{p}}$ (1/32 sec)
3WW1	10	17	115	-61	6.2	0.24	0.64	0.84
3WW2	14	14	93	-28	5.6	0.33	0.42	0.68
3WW3	18	14	96	-24	5.6	0.43	0.56	0.70
3WW4	19	16	109	-21	5.6	0.45	0.60	0.80
3WW5	23	16	115	-18	5.7	0.55	0.60	0.84
3WW6	26	22	148	-38	5.5	0.62	0.76	1.08
3WW7	16	16	121	-36	6.6	0.38	0.54	0.89
5WW1	26	19	131	-17	5.5	0.62	0.71	0.96
5WW2	41	20	137	-4	4.8	0.98	0.79	1.00
5WW3	38	20	148	-2	5.5	0.91	0.90	1.08
5WW4	16	20	126	-30	5.5	0.38	0.69	0.92
5WW5	15	21	149	-33	6.4	0.36	0.71	1.09
5WW6	36	20	198	-12	8.1	0.86	0.83	1.45
5WW7	33	18	150	-22	6.5	0.79	0.76	1.10
3EW1	-21	8.7	0	-67	5.3	-0.50	-0.39	-0.49
3EW2	-22	9.3	0	-69	5.0	-0.53	-0.39	-0.50
3EW3	-23	8.9	-2	-69	5.2	-0.55	-0.40	-0.50
3EW4	-20	7.5	0	-65	6.0	-0.48	-0.41	-0.48
3EW5	-23	8.9	6	-74	5.7	-0.55	-0.43	-0.54
5EW1	-15	7.5	4	-54	5.2	-0.36	-0.32	-0.39
5EW2	-20	7.4	-2	-54	4.6	-0.48	-0.34	-0.39
5EW3	-22	9.0	2	-64	4.7	-0.53	-0.39	-0.47
5EW4	-22	7.8	-2	-71	6.3	-0.53	-0.42	-0.52
5EW5	-24	8.7	0	-81	6.5	-0.57	-0.42	-0.59
3SW1	-31	19	60	-174	7.5	-0.74	-0.63	-1.27
3SW2	-29	20	86	-148	6.0	-0.69	-0.64	-1.08
3SW3	-15	13	30	-146	10.1	-0.36	-0.44	-1.07
3SW4	-11	7.2	20	-57	6.4	-0.26	-0.24	-0.42
5SW1	19	22	134	-89	5.2	0.45	0.65	0.98
5SW2								
3NW1	-28	10	-2	-80	5.2	-0.67	-0.50	-0.58
3NW2	-35	14	4	-140	7.5	-0.84	-0.72	-1.02
INT	-12	6.1	9	-49	6.1	-0.29	-0.25	-0.36
OH-U	90	21	327	-7	11.3			
OH-L	34	19	142	-23	5.7	0.81	0.86	1.04
WR1A	-8	27	78	-242	8.7	-0.19	-0.73	-1.77
WR1B	-16	27	80	-256	8.9	-0.38	-0.86	-1.87
WR1C	-17	21	79	-187	8.1	-0.41	-0.64	-1.37
WR1E	7	19	102	-63	5.0	0.17	0.40	0.75
WR1F	-7	14	66	-85	5.6	-0.17	-0.28	-0.62
WR2C	6	16	72	-84	4.9	0.14	-0.33	-0.61
WR2E	20	12	97	-18	6.4	0.48	0.42	0.71
WR3A	6	6.3	49	-46	8.2	0.14	0.15	0.36
WR3B	5	6.3	44	-46	8.1	0.12	0.13	0.32
WR3C	4	6.2	55	-45	8.2	0.10	0.13	0.40
WR3D	2	7.9	52	-41	6.3	0.05	0.18	0.38
WR3E	5	6.8	46	-23	6.0	0.12	0.18	0.34
WR4C	-9	4.6	19	-32	5.0	-0.22	-0.18	-0.23
ER1A	-25	11	9	-116	8.3	-0.60	-0.45	-0.85
ER1B	-33	13	-2	-114	6.2	-0.79	-0.55	-0.83
ER1C	-34	12	0	-155	10.1	-0.81	-0.71	-1.13
ER2A	-20	11	7	-85	5.9	-0.48	-0.44	-0.62
ER2B	-22	11	11	-97	6.8	-0.53	-0.48	-0.71
ER3A	-4	9.4	14	-89	9.0	-0.10	-0.48	-0.65
ER3B	-15	9.3	45	-68	6.5	-0.36	-0.35	-0.50

Duration 1024 seconds. $\bar{u}_{10} = 8.3\ ms^{-1}$; $\bar{u}_5 = 6.6\ ms^{-1}$; $\bar{u}_3 = 5.6\ ms^{-1}$

$\bar{\beta} = 220^o$. $\sigma_{u_{10}} = 2.1\ ms^{-1}$; $\sigma_{u_5} = 1.8\ ms^{-1}$; $\sigma_{u_3} = 1.7\ ms^{-1}$

$\bar{\theta} = 248^o$. $\hat{u}_{10} = 14.9\ ms^{-1}$; $\hat{u}_5 = 13.5\ ms^{-1}$; $\hat{u}_3 = 12.1\ ms^{-1}$

Printed for Her Majesty's Stationery Office by
Chas F. Thorn and Son Ltd. Erith, Kent 3.2M 2/76 1952

Current papers – recent issues

CP53/75	A graphical method of predicting side-sway in the design of multi-storey buildings.	B H WOOD and E H ROBERTS
CP54/75	Field measurements of the sound insulation of cavity party walls of aerated concrete blockwork in local authority housing.	W A UTLEY
CP55/75	An international survey of research into road traffic noise.	W G SCHOLES and L C FOTHERGILL
CP56/75	Energy conservation: a study of energy consumption in buildings and possible means of saving energy in housing.	B A AKAM and P LAWSON
CP57/75	Construction site noise.	A A B MUSANNIF
CP58/75	Thermic boring.	D C TEYCHENNE
CP59/75	High alumina cement concrete: research and results.	J A CHARLES
CP60/75	Strains developed in two rockfill dams during construction.	N P SKINNER
CP61/75	Research on windows at Princes Risborough Laboratory.	R J MAINSTONE
CP62/75	Properties of materials at high rates of straining or loading.	S G SAMUELS
CP63/75	Some properties of the Gault Clay from the Ely–Ouse Essex water tunnel.	N J KING and G A SMITH
CP64/75	Problems of wood waste.	D L HILLS
CP65/75	Premixed glass fibre reinforced cement.	A A B MUSANNIF
CP66/75	Quieter demolition techniques.	P NASH and R A YOUNG
CP67/75	The performance of the sprinkler in the extinction of fire.	K ALSOP and A J LOCKWOOD
CP68/75	A research management course.	A J BUTLER
CP69/75	Construction safety research at BRE.	P F THORNE
CP70/75	Drag reduction in fire-fighting.	D C TEYCHENNE
CP71/75	Long-term research into the characteristics of high alumina cement concrete.	H G MIDGLEY and A MIDGLEY
CP72/75	The conversion of high alumina cement.	S G SAMUELS and J E CHENEY
CP73/75	Long-term heave of a building on clay due to tree removal.	D F PURSLOW
CP74/75	The assurance of quality provided by certain British Standards concerned with timber products.	E N ZEMAN and WENDY LIGHT
CP75/75	Availability of sunshine.	M A HUMPHREYS
CP76/75	Field studies of thermal comfort compared and applied.	R A YOUNG and P NASH
CP77/75	The testing of sprinkler installations.	P NASH and R A YOUNG
CP78/75	The testing of sprinklers.	P NASH
CP79/75	The essentials of sprinkler and other water spray fire protection systems.	P L WALTON and A J MAJUMDAR
CP80/75	Cement-based composites with mixtures of different types of fibres.	P F THORNE
CP81/75	The strength of fire extinguishers.	P NASH
CP82/75	Some design aspects of fire extinguishers.	P L MINKLEY
CP83/75	Work by the Fire Research Station on the control of smoke in covered shopping centres.	R G WHITE
CP84/75	The durability of glues for plywood manufacture.	J LEMESSANY and M A CLAPP
CP85/75	Resource inputs to new construction – the labour requirements of hospital building.	D F PURSLOW
CP86/75	Results of stake tests on wood preservatives (Progress report b 1974).	A D M PENMAN and J A CHARLES
CP87/75	The quality and suitability of rockfill used in dam construction.	J M BAKER, E R MILLER, J W W MORGAN and J G SAVORY
CP88/75	Research in wood protection at the Princes Risborough Laboratory 1973 and 1974.	C A PRICE
CP89/75	The decay and preservation of natural building stone.	J B DICK
CP90/75	Building: research and future trends.	J F EDEN
CP91/75	A review of accidents in the construction industry.	A F BRAVERY
CP92/75	Microbiological assay of chemicals for the protection of wood.	J K CAREY
CP93/75	Notes on the isolation and characterisation of wood-inhabiting fungi.	M A ALI, A J MAJUMDAR and B SINGH
CP94/75	Properties of glass fibre cement – the effect of fibre length and content	

continued

Current papers — recent issues

CP95/75	Evacuation of buildings – some effects of changes in performance standards	S J MELUISH and R BALDWIN
CP96/75	An analysis of evacuation times and the movement of crowds in buildings	S J MELUISH and S BOOTH
CP97/75	A survey of decay, insect attack and moisture contents in timber components in Scottish housing	J C BEECH and P L NEWMAN
CP98/75	The performance of a foam-sprinkler installation on simulated oil-rig fires	R A YOUNG and J G CORRIE
CP99/75	Accuracy of in-situ concrete	R F THOROGOOD
CP100/75	Deformations and stresses in rockfill over a rigid culvert	A D M PENMAN and J A CHARLES
CP1/76	Wind loads on low-rise buildings – effects of roof geometry	K J EATON, J R MAYNE and N J COOK